Modélisation de la variabilité climatique et de ses liens avec la cryosphère dans les Hautes Montagnes d'Asie

Mickaël Lalande

PhD Student 2019-2022

Encadrants : Martin Ménégoz et Gerhard Krinner

Membres du comité : Frédérique Cheruy (référent HDR) et Isabelle Gouttevin

Institut des Géosciences de l'Environnement (IGE, Grenoble, France)

Comité de thèse 1ère année — 10/09/2020

1. Mon début de thèse
2. Introduction High Mountain of Asia
3. Analyse des biais dans LMDZ (CMIP6)
4. Analyse multi-modèle CMIP6
5. Lien des biais avec la topographie
6. Paramétrisation sous-maille de la topographie
7. Autres prospectives
8. Conclusions sur le déroulement de la thèse

Mon début de thèse

Cursus universitaire

Expériences personnelles

3 mois en Nouvelle-Zélande

1 an en VVT au Japon
→ Anglais

Auto-entreprise développement web
→ programmation

Passion pour la Science et l'Environnement

Expériences professionnelles

Prépa PCSI/PSI

Supméca Paris
→ ~~ingénieur~~

L3 STPE/Physique
-> recherche plus fondamentale

Stages glaciologie + astrophysique

Stage atmosphère

Master ACSC
→ atmosphère / cryosphère / modélisation

Stage océan + machine learning
→ complémentaire à ma formation
→ soumission d'un papier

Projet de thèse autour de la modélisation atmosphère/cryosphère et du réchauffement climatique

CMIP6 — vers CMIP7

1ère année

- Bibliographie
- Prise en main du LMDZ
- Novembre : réunion atmosphère/orchidée
- Décembre : formation LMDZ
- 1ère simus + comparaisons

2ème année

- Paramétrisation sous-maille
- Développement LMDZ (collaboration avec l'IPSL)
- Comparaison CMIP6
- Terrain Himalaya ?
- Visite BSC ?

3ème année

- Projections futures (+ avec correction de biais ?)
- MAR dans LMDZ ?
- Finalisation de la thèse
- Ecriture du mémoire

après...

- Post-doc à l'étranger
- Continuer dans la recherche
- Continuer de me spécialiser dans la modélisation atmosphère/cryosphère

Trainings and Meetings

01/10/2019
Start PhD

23-25/10/2019
Formation Fortran Base

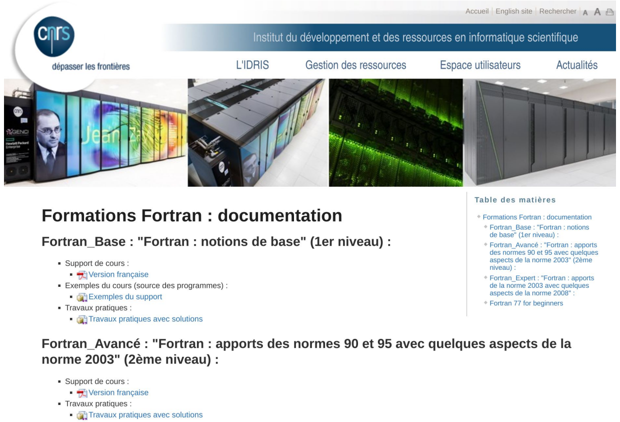

14-15/11/2019
Journée de Modélisation des Surfaces Continentales

26-29/11/2019
Formation Fortran Avancé

9-11/12/2019
LMDZ training course

13/01/2020
PEDALONS zoom

14-17/01/2020
IPSL running environment + ORCHIDEE training course

Introduction High Mountain of Asia

High Mountain Asia (HMA): Introduction

- The Tibetan Plateau (TP) region is the world's highest plateau (average elevation 4000m) ➝ considerable influence on regional and global climate. (Orsolini et al., 2019)
- Directly sustain the livelihoods of 240 million people in the mountain and hills of the Hindu Kush Himalaya. (Sharma et al., 2019)
- Two distinct climatic regimes:
  - winter westerly disturbances ➝ 50 % of the precipitation over the western Himalaya and Hindu Kush mountains
  - central and eastern Himalayan mountains receiving major part (up to 80%) of annual precipitation during the Indian summer monsoon months (June-September). (Bookhagen and Burbank, 2010)

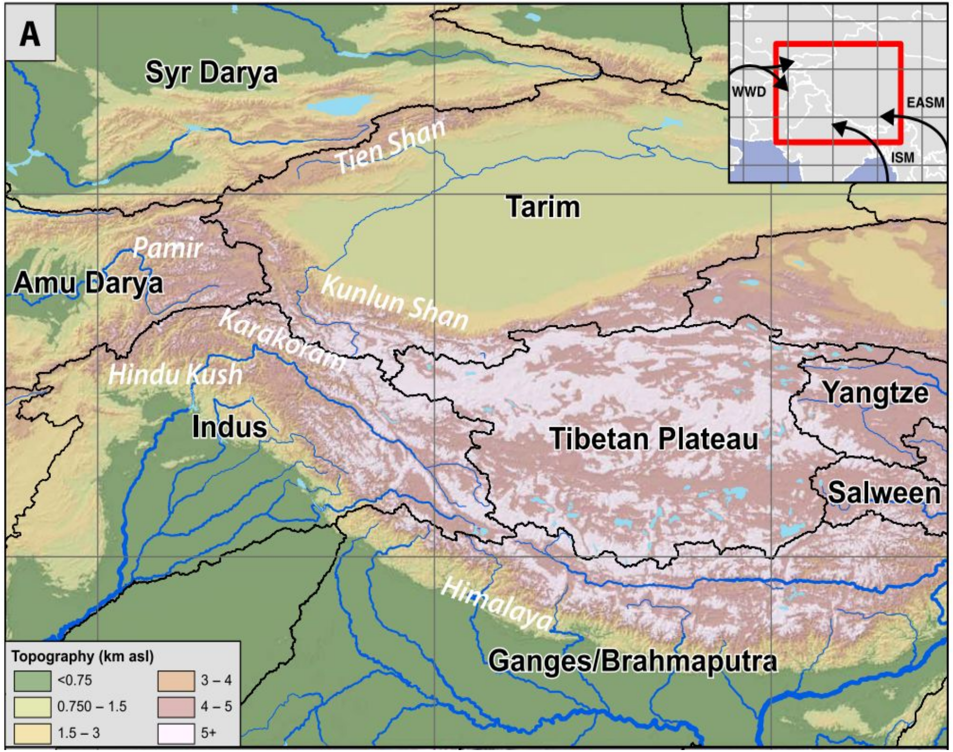

Smith and Bookhagen (2018), Fig. 1A

High Mountain Asia (HMA): station observations

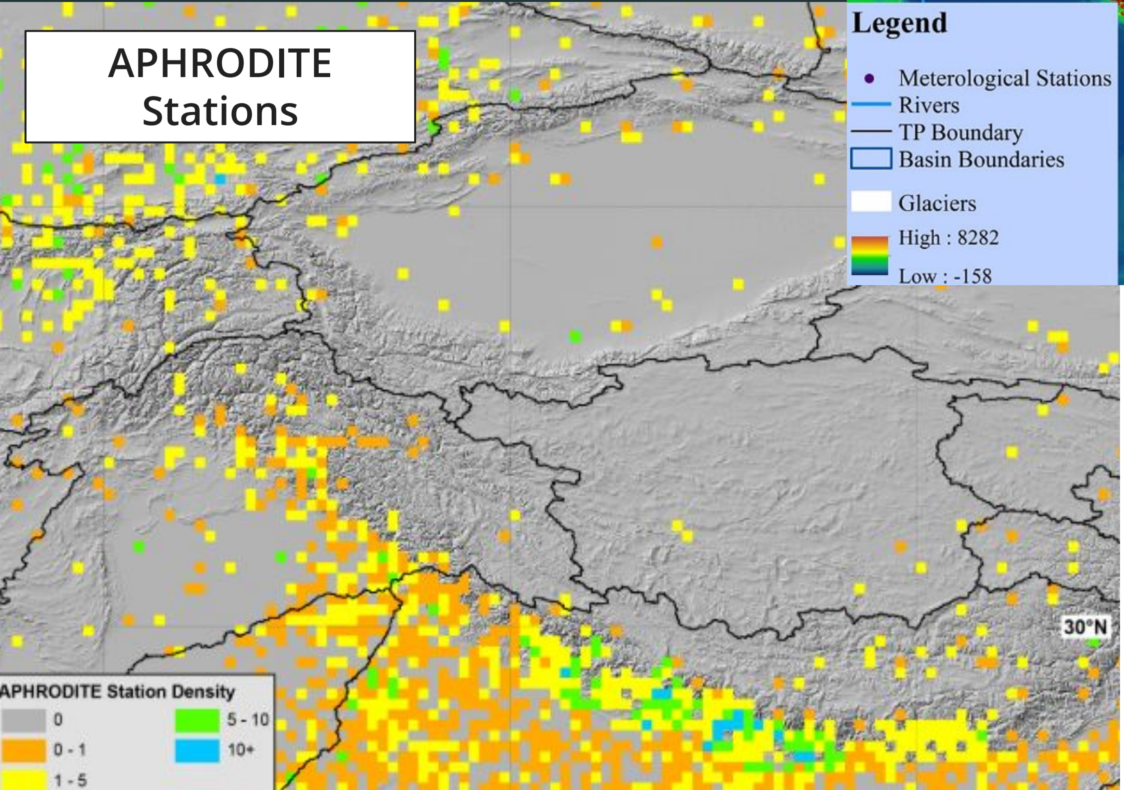

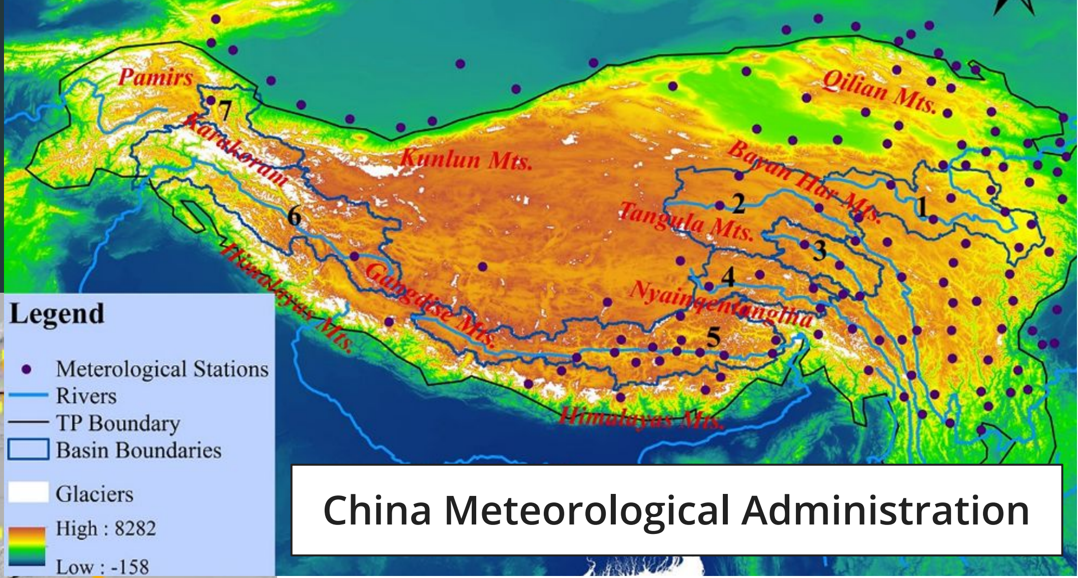

Li et al. (2018), Fig. 1

- Illustrates the low station density in the core of HMA (Tibetan Plateau)
- The highest elevations are severely under-represented
- Almost exclusively measure rainfall (there exist very few snow monitoring stations in HMA)

Smith and Bookhagen (2018), Fig. S1

Analyse des biais dans LMDZ (CMIP6)

Snow bias in IPSL model CMIP5 versus CMIP6

WANG ET AL.: ORCHIDEE SNOW MODEL EVALUATION

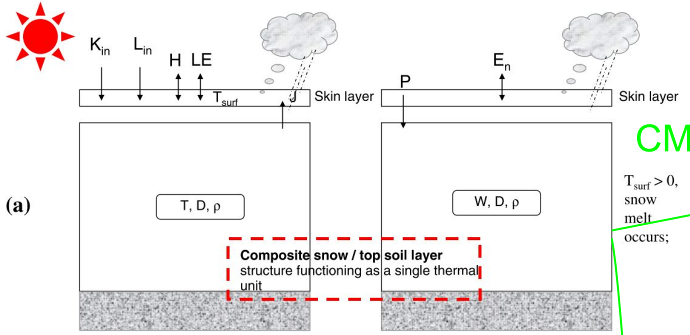

K_{in} (short wave radiation), **L_{in}** (longwave radiation), **H** (sensible heat flux), **LE**(latent heat flux), **J** (conduction heat flux), **W** (SWE), **D** (snow depth), **ρ** (fixed snow density 330) , **P** (precipitation), **E_n** (evaporation), **T**(snow temperature), **Tsurf**(skin layer temperature)

CMIP5

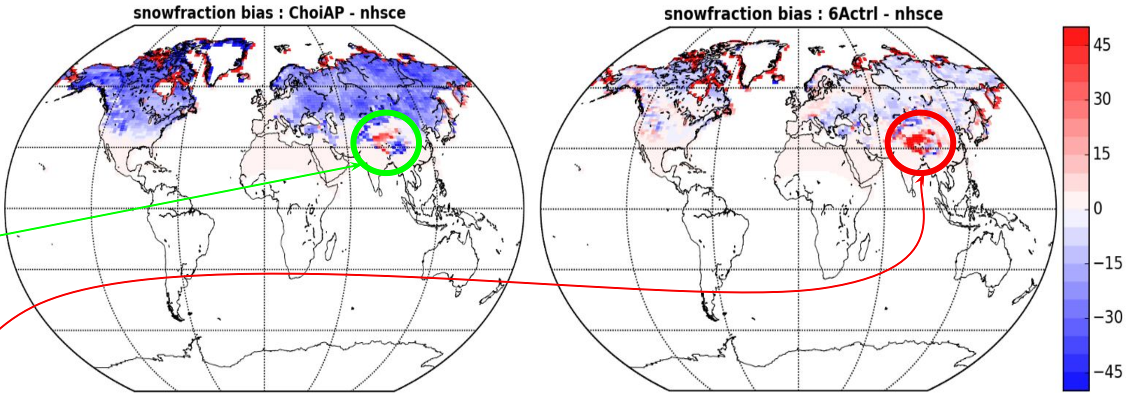

Cheruy et al. (2020), Fig. 6

CMIP6

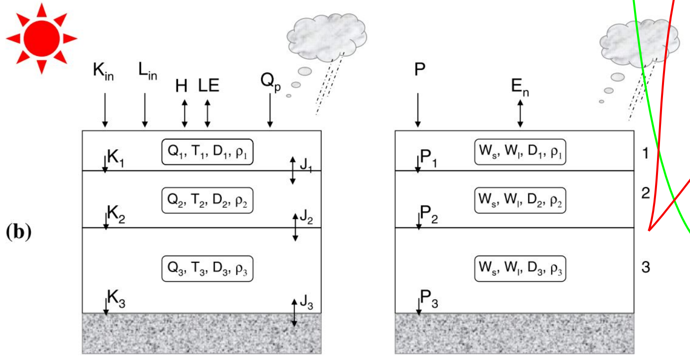

K_{in} (short wave radiation), **L_{in}** (longwave radiation), **H** (sensible heat flux), **LE**(latent heat flux), **J** (conduction heat flux), **Q** (snow layer heat content), **Q_p**(advective heat from rain and snow), **W** (snow layer SWE), **W_l** (snow layer liquid water content), **D** (snow layer depth), **ρ** (snow layer density) , **P** (precipitation), **E_n** (evaporation)

Wang et al. (2013), Fig. 1

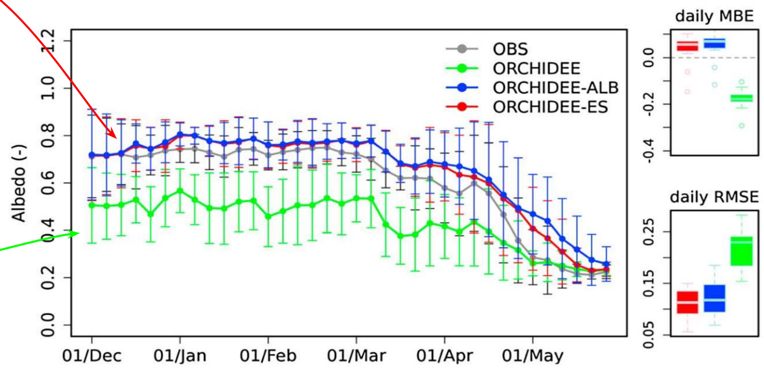

Wang et al. (2013), Fig. 5

IPSL-CM6A-LR: Historical, AMIP, land-hist / IPSL-CM6A-ATM-HR bias

Snow cover bias

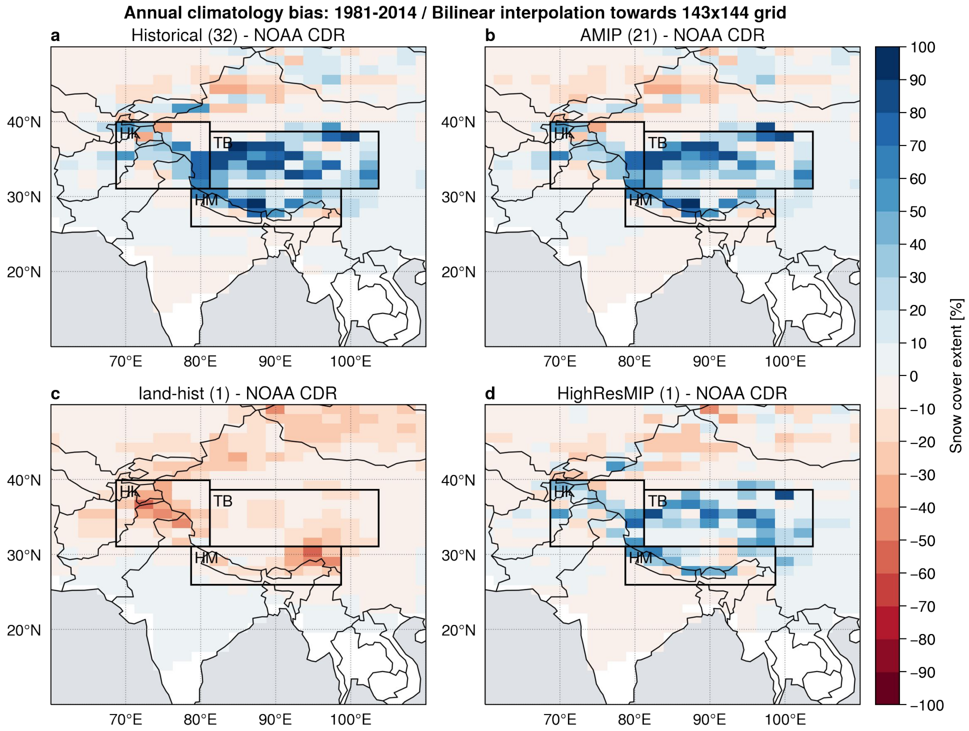

Temperature bias

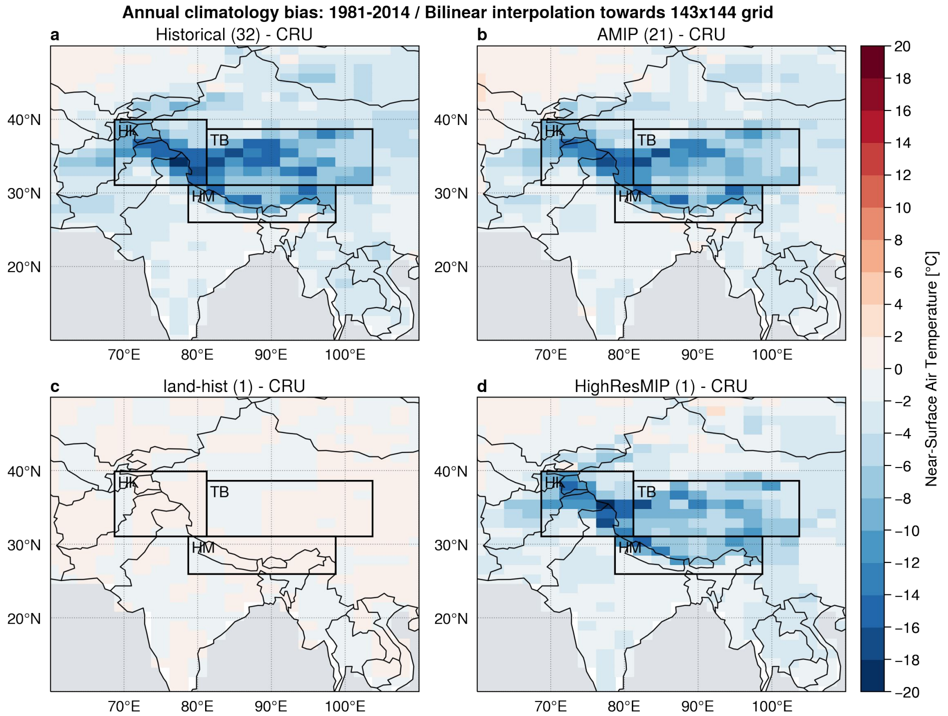

Air Temperature zonal means bias global versus HMA

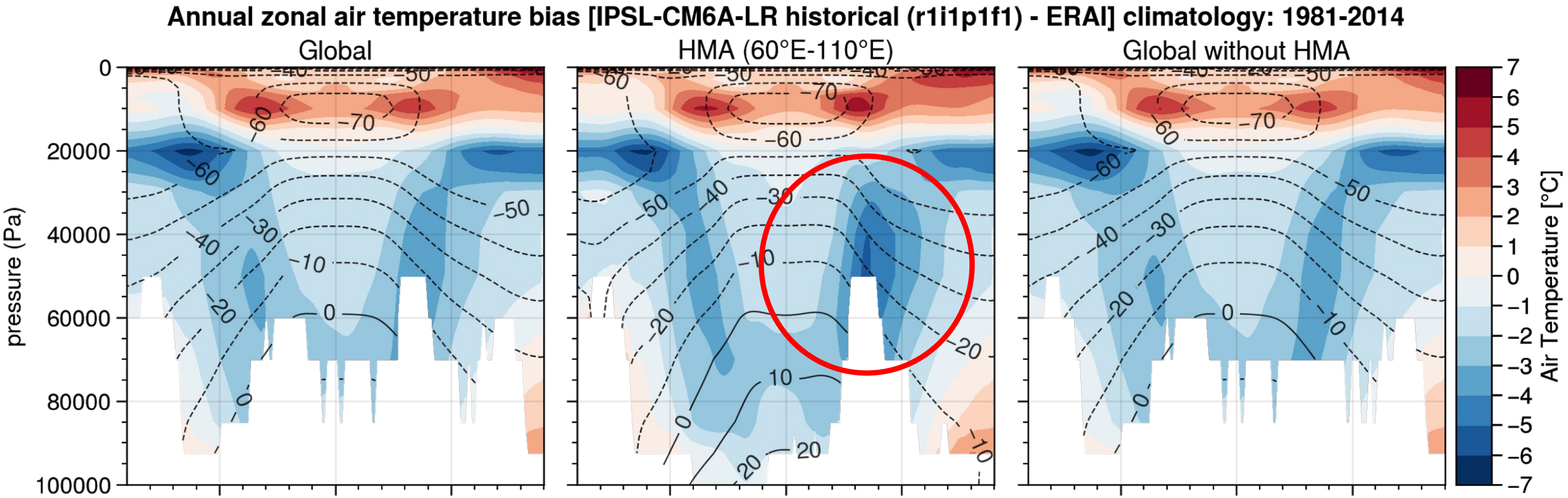

- Cold bias in troposphere and hot bias in stratosphere
- Cold bias of air temperature not restricted to HMA!
- HMA seems to amplify this bias
- The bias is reduced in HighResMIP

Adapted from from Boucher et al., Fig. 3 (2020)

Nudged versus not nudged: snow cover* (tropo bias)

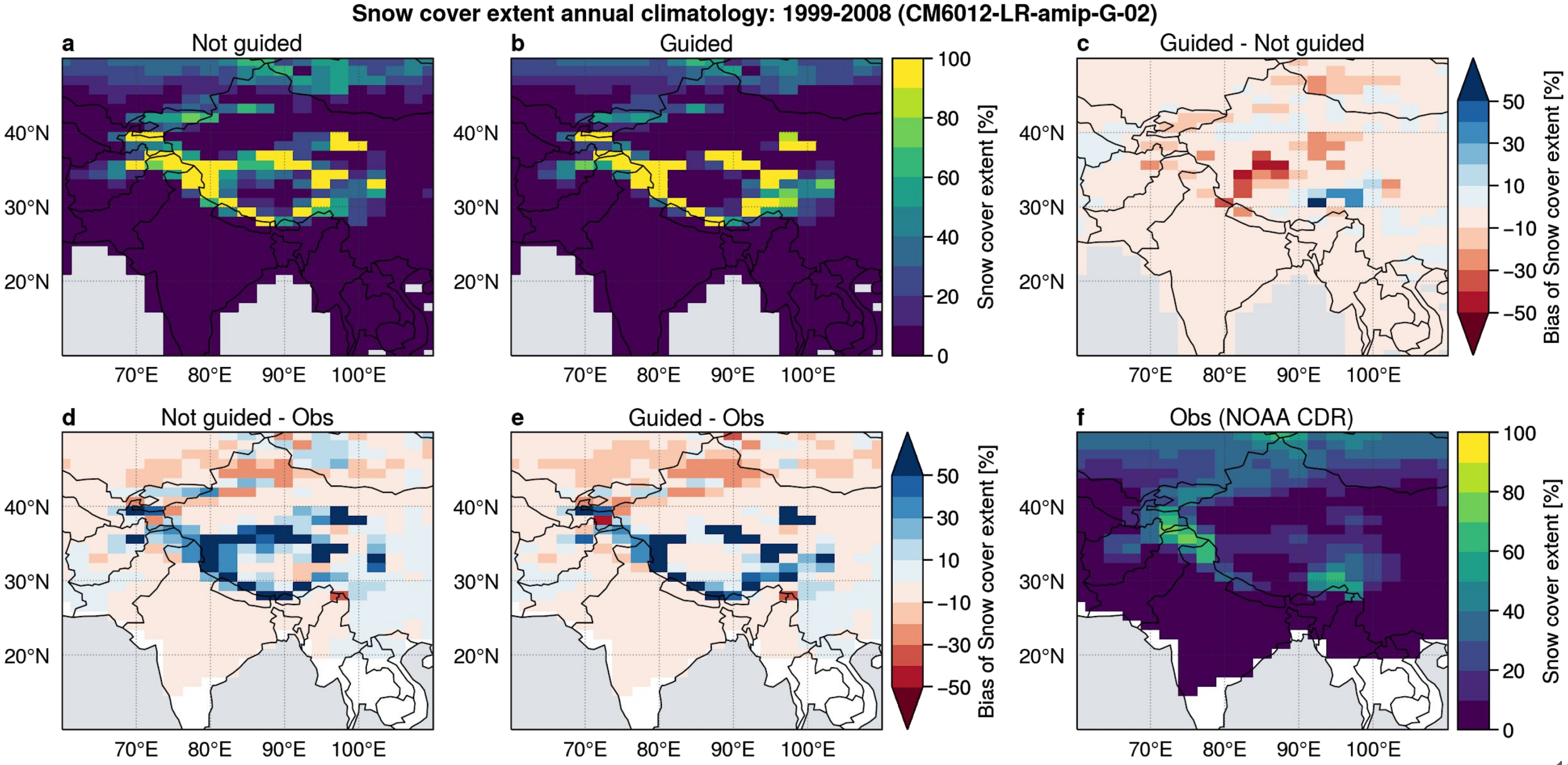

* Simulation: Frédérique Cheruy

Analyse multi-modèle CMIP6

CMIP6 other models: Near-Surface Air Temperature bias

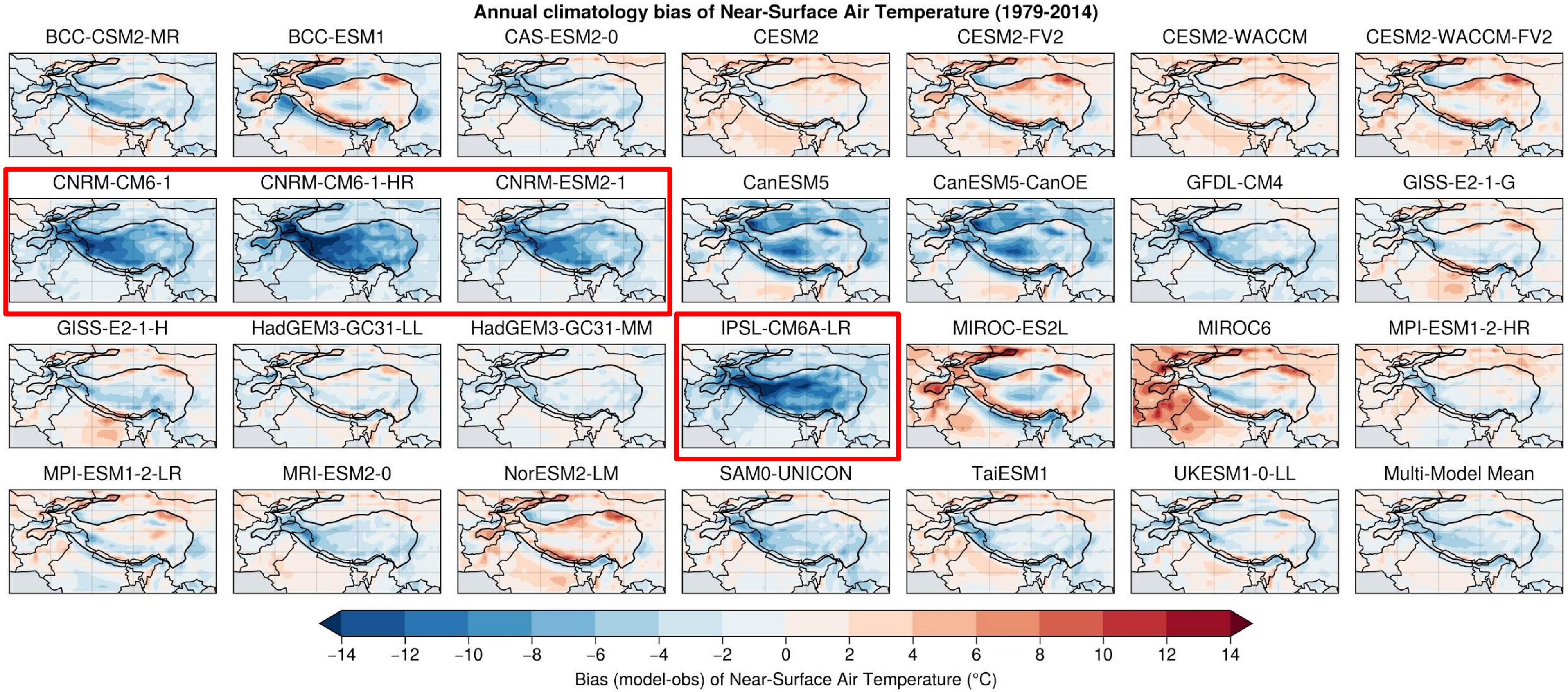

CMIP6 other models: Snow Cover bias

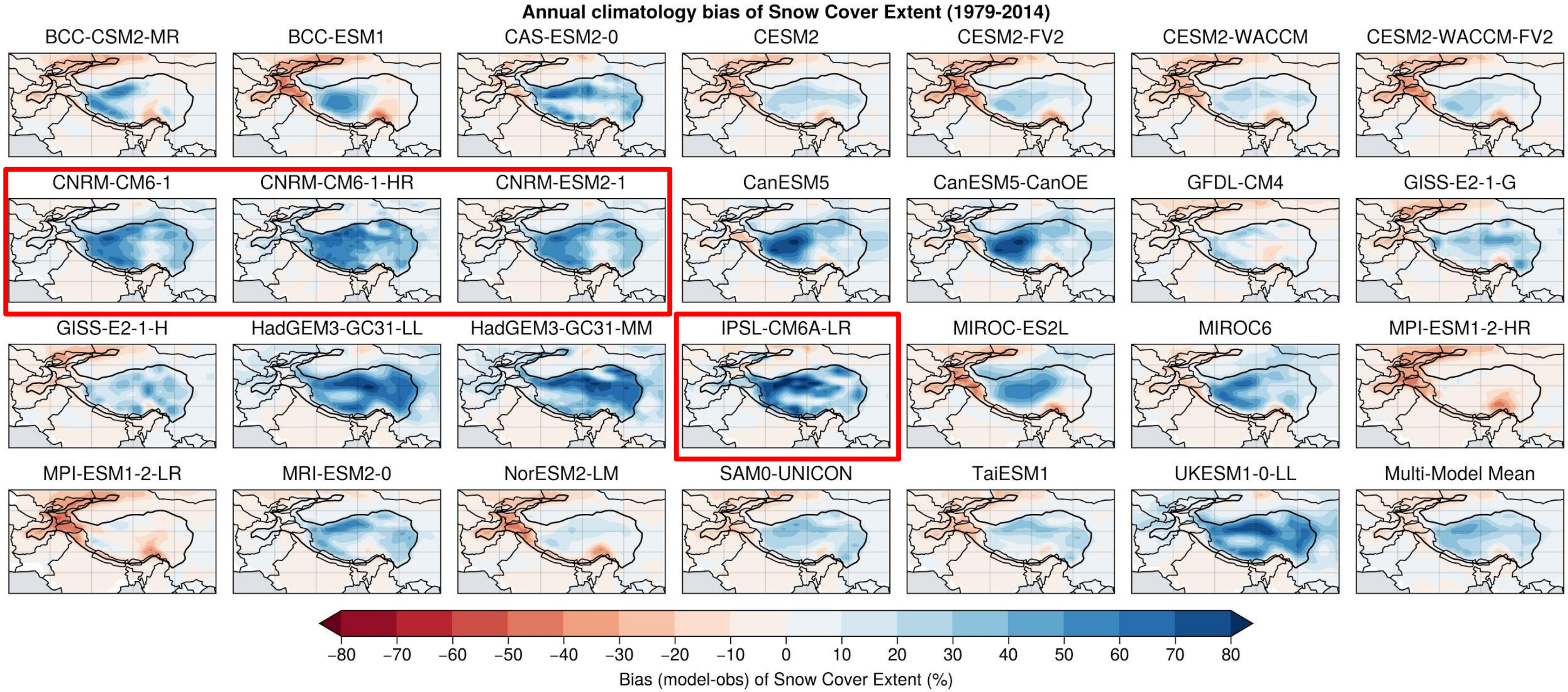

CMIP6 other models: Total Precipitation bias

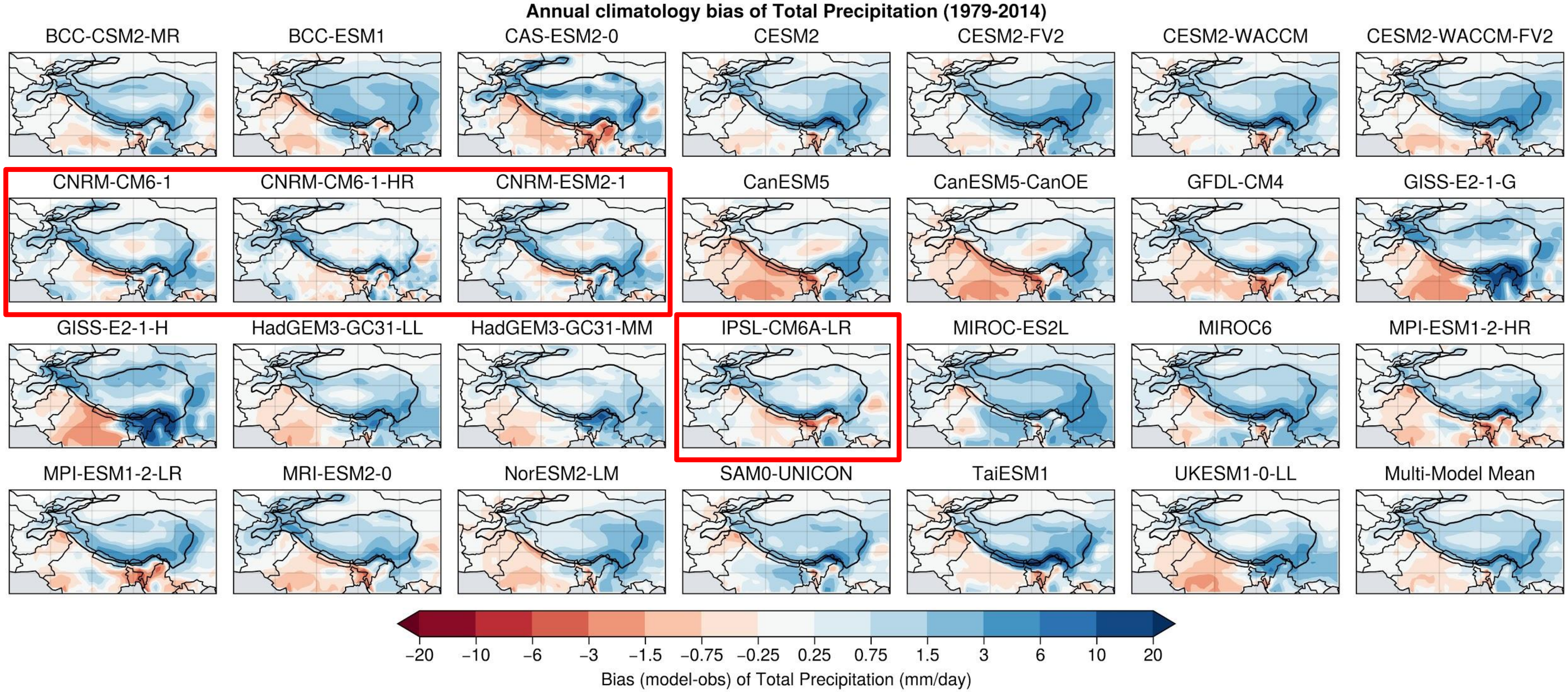

CMIP6 other models: Near-Surface Air Temperature metrics

Sorted by annual RMSE

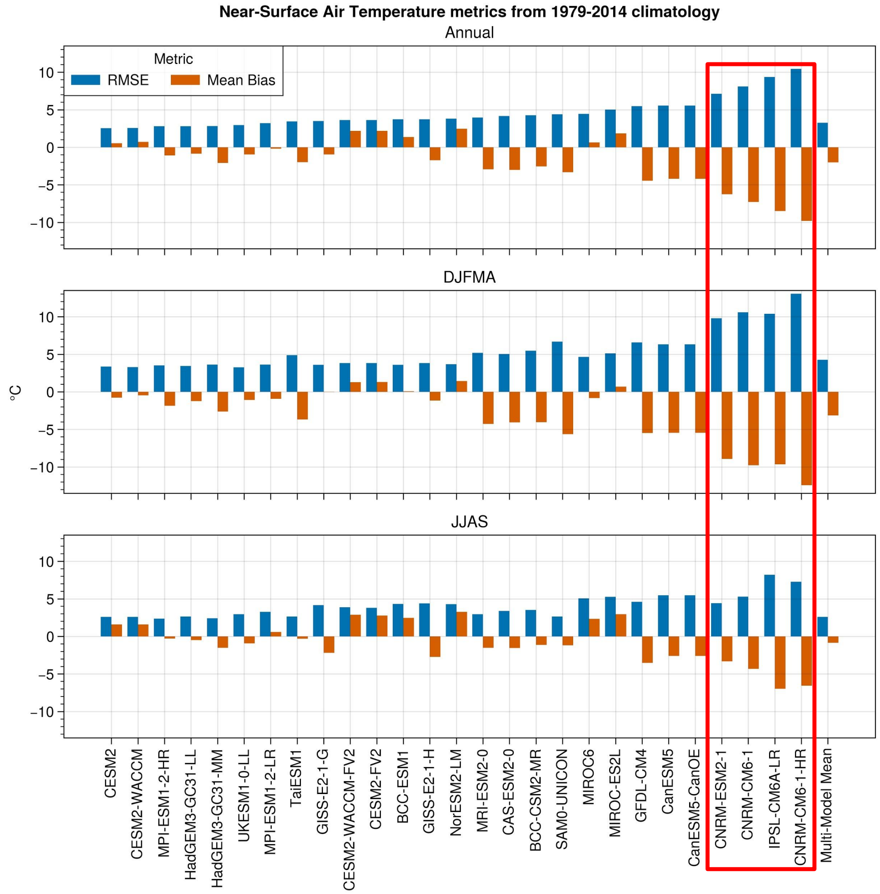

Sorted by resolution

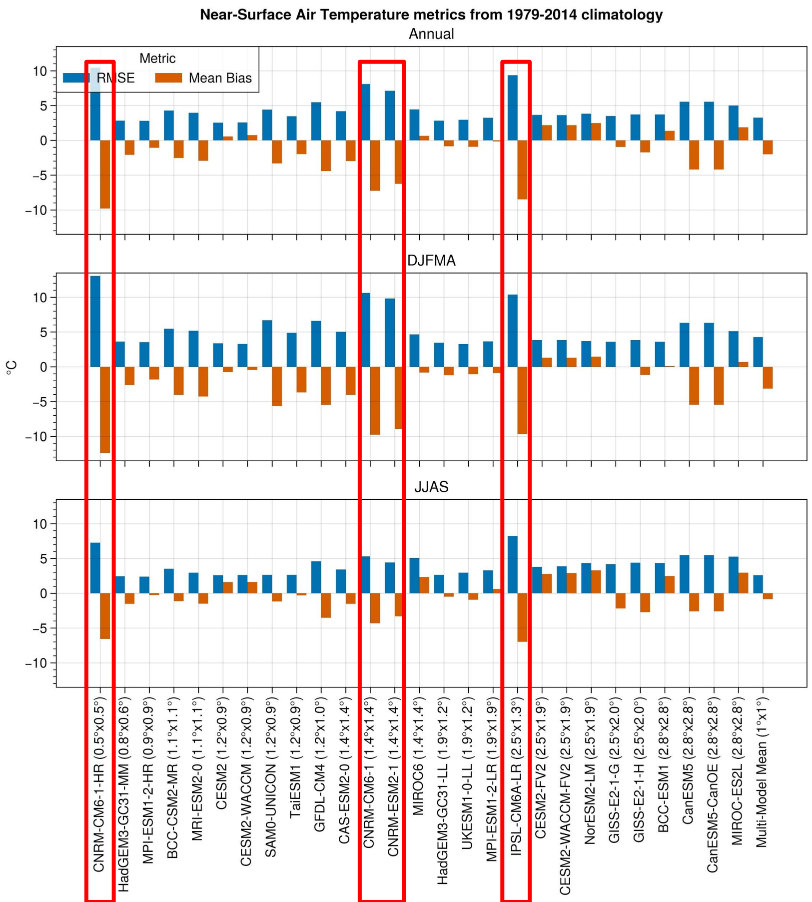

CMIP6 other models: spatial correlations

Spatial correlation of bias over HMA from 1979-2014 climatology

		BCC-CSM2-MR	BCC-ESM1	CAS-ESM2-0	CESM2	CESM2-FV2	CESM2-WACCM	CESM2-WACCM-FV2	CNRM-CM6-1	CNRM-CM6-1-HR	CNRM-ESM2-1	CanESM5	CanESM5-CanOE	GFDL-CM4	GISS-E2-1-G	GISS-E2-1-H	HadGEM3-GC31-LL	HadGEM3-GC31-MM	IPSL-CM6A-LR	MIROC-ES2L	MIROC6	MPI-ESM1-2-HR	MPI-ESM1-2-LR	MRI-ESM2-0	NorESM2-LM	SAM0-UNICON	TaiESM1	UKESM1-0-LL
Annual	tas/snc	−0.51	−0.45	−0.21	−0.02	−0.29	0.01	−0.29	−0.5	−0.39	−0.47	−0.53	−0.53	−0.4	−0.36	−0.35	−0.28	0.16	−0.62	−0.71	−0.58	0.09	−0.23	−0.16	−0.25	−0.18	−0.09	−0.17
	tas/pr	−0.09	−0.22	−0.08	−0.18	−0.21	−0.19	−0.22	0.02	−0.05	−0.02	0.16	0.16	−0.16	−0.11	−0.04	−0.04	−0.07	0.02	−0.07	0.02	−0.37	−0.35	−0.24	−0.26	−0.12	−0.14	−0.02
	snc/pr	0.18	0.48	0.41	−0.22	−0.05	−0.18	−0.04	−0.23	−0.38	−0.23	−0.06	−0.06	0.04	−0.02	0.03	0.05	−0.04	0.06	0.01	−0.31	−0.12	0.1	−0.22	0.13	0.1	0.01	−0.03
DJFMA	tas/snc	−0.52	−0.48	−0.3	−0.31	−0.49	−0.28	−0.49	−0.5	−0.24	−0.52	−0.37	−0.37	−0.45	−0.34	−0.33	−0.14	0.17	−0.51	−0.69	−0.55	−0.12	−0.36	−0.18	−0.36	−0.41	−0.25	−0.03
	tas/pr	−0.21	−0.17	−0.07	−0.31	−0.27	−0.33	−0.29	−0.02	−0.02	−0.02	−0.03	−0.03	−0.44	−0.17	−0.09	−0.01	−0.14	−0.12	0.11	−0.1	−0.38	−0.35	−0.24	−0.27	−0.13	−0.2	−0.11
	snc/pr	0.31	0.74	0.08	−0.35	−0.19	−0.32	−0.18	−0.41	−0.5	−0.44	0.24	0.24	0.11	−0.04	−0.07	0.12	0.09	−0.13	0.1	−0.41	−0.07	−0.01	−0.22	0.04	−0.03	0.08	0.02
JJAS	tas/snc	−0.43	−0.4	−0.14	0.22	−0.08	0.22	−0.1	−0.49	−0.54	−0.43	−0.62	−0.62	−0.14	−0.48	−0.39	−0.33	−0.05	−0.74	−0.53	−0.43	0.24	−0.01	0.04	−0.16	0.24	0.15	−0.32
	tas/pr	−0.03	−0.28	−0.09	−0.08	−0.18	−0.11	−0.18	−0.02	−0.08	−0.03	0.23	0.23	0.08	−0.08	−0.02	−0.02	0	0.13	−0.28	−0.13	−0.4	−0.39	−0.08	−0.28	−0.12	−0.19	0
	snc/pr	−0.12	0.27	0.45	0.06	0.12	0.04	0.13	−0.12	−0.21	−0.1	−0.13	−0.13	−0.13	−0.01	0.02	−0.01	−0.07	−0.02	0.21	−0.07	−0.04	0.05	−0.1	0.24	0.24	0.06	−0.07

“Cold bias” over Tibetan Plateau

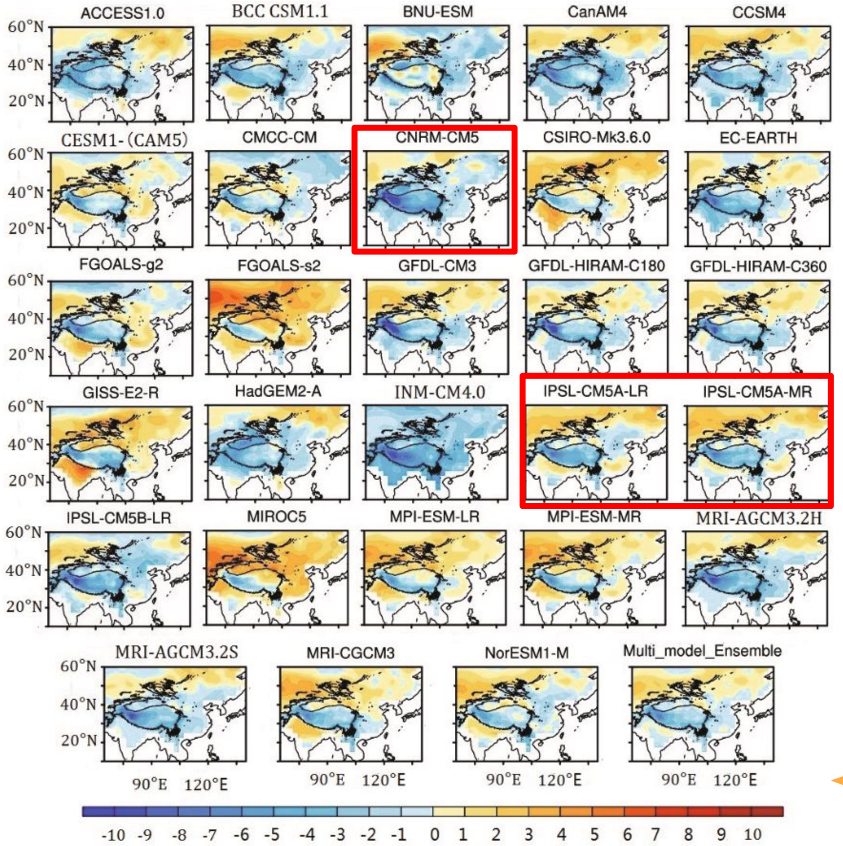

Fig. 2. Annual mean T_{as} (°C) differences between various models and CRU data averaged during 1979–2005. All air temperature values in the models have been corrected to real elevation at a resolution of 2.5°×2.5°.

- The large cold biases are located in the mountainous areas, such as the Rocky Mountains, the Tibetan Plateau, the Andes, Greenland, and Antarctica, and seem to be proportional to the topographic height. (Mao and Robock, 1998 — First AMIP experiments)
- These cold biases are partly attributable to the simulation of excess precipitation in these regions (Lee & Suh, 2000). The lack of high-elevation observation stations in the CRU data may also be partly responsible for the apparent cold bias of the model (Gu et al., 2012). (Wang et al., 2013 — regional climate model RegCM)
- This feature may imply a common deficiency in the representation of snow–ice albedo in the diverse models. It appears that the systematic bias and the significant problems over the mountain regions (e.g., the Tibetan Plateau) still remain in the CMIP5 models. (Su et al., 2013)
- GCMs show predominant cold biases in T500, which may be caused by penetration of dry and cold air from the deserts of western Asia due to an overly smoothed representation of topography west of the TP (Boos and Hurley, 2013). (Xu et al., 2017 — CMIP5)
- The results suggest that improvements in the **parameterization of the area of snow cover**, as well as the boundary layer, and hence surface turbulent fluxes, may help to reduce the cold bias over the TP in the models. (Chen et al., 2017 — surface energy budget CMIP5)
- Others: Salunke et al. (2019)., etc.

Lien des biais avec la topographie

Problem with elevation?

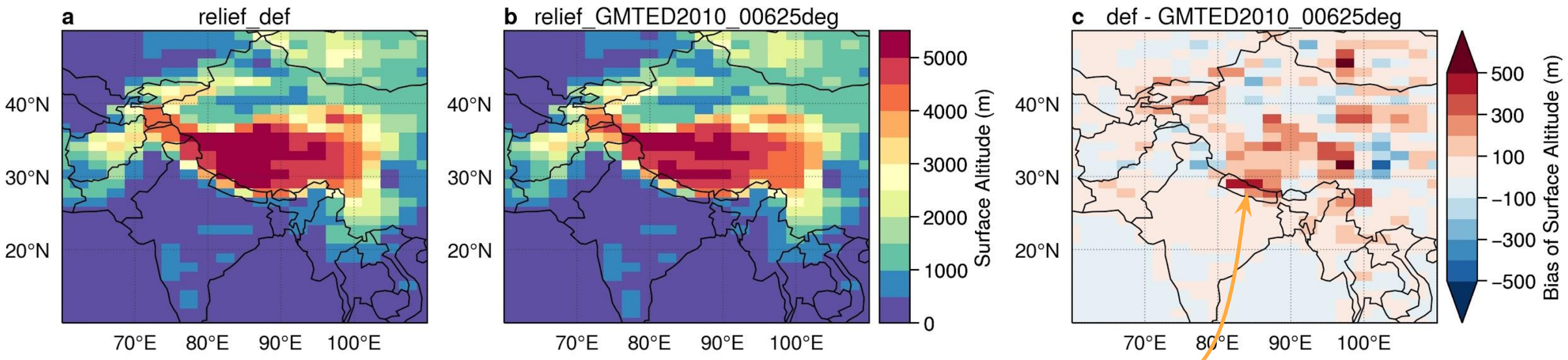

Original file of elevation has more than 500 m differences locally!

Already targeted in 2018 : https://lmdz.lmd.jussieu.fr/utilisateurs/reunion-utilisateurs/2018/jlmdz2018-sepulchre.pdf

→ 2 climatological experiments of 10 years with original and new topography (GMTED2010)

Problem with elevation?

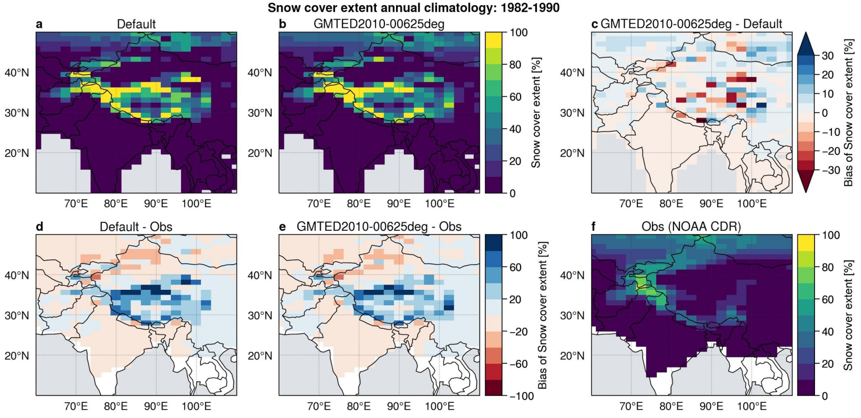

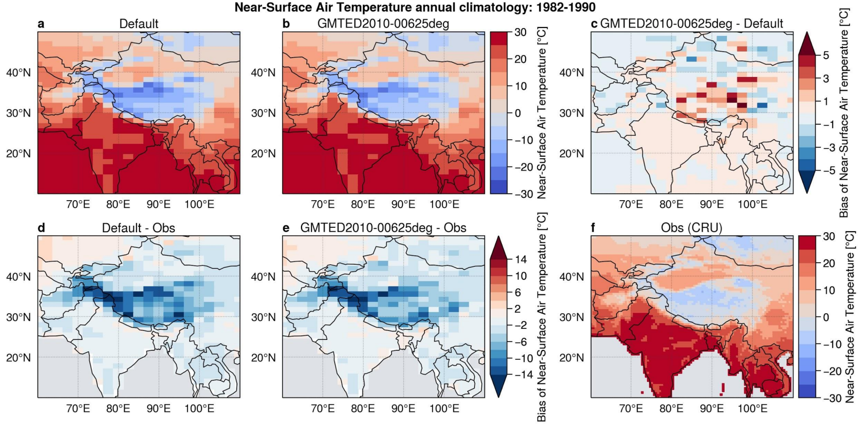

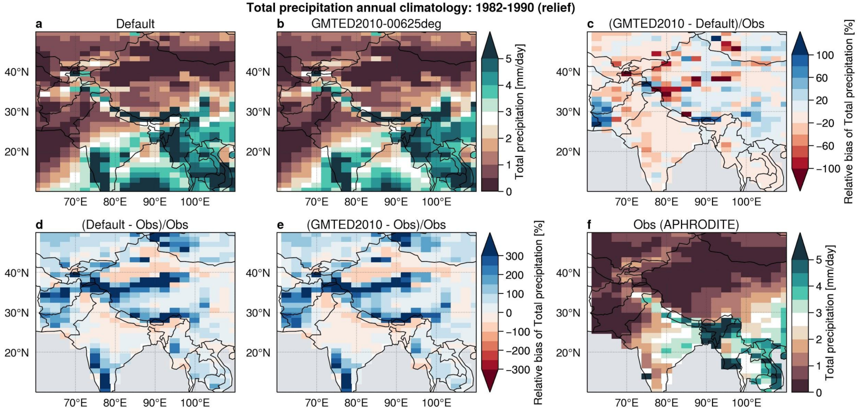

- Some improvements around the area of high elevation differences
  - Bias still present!

Link with orography?

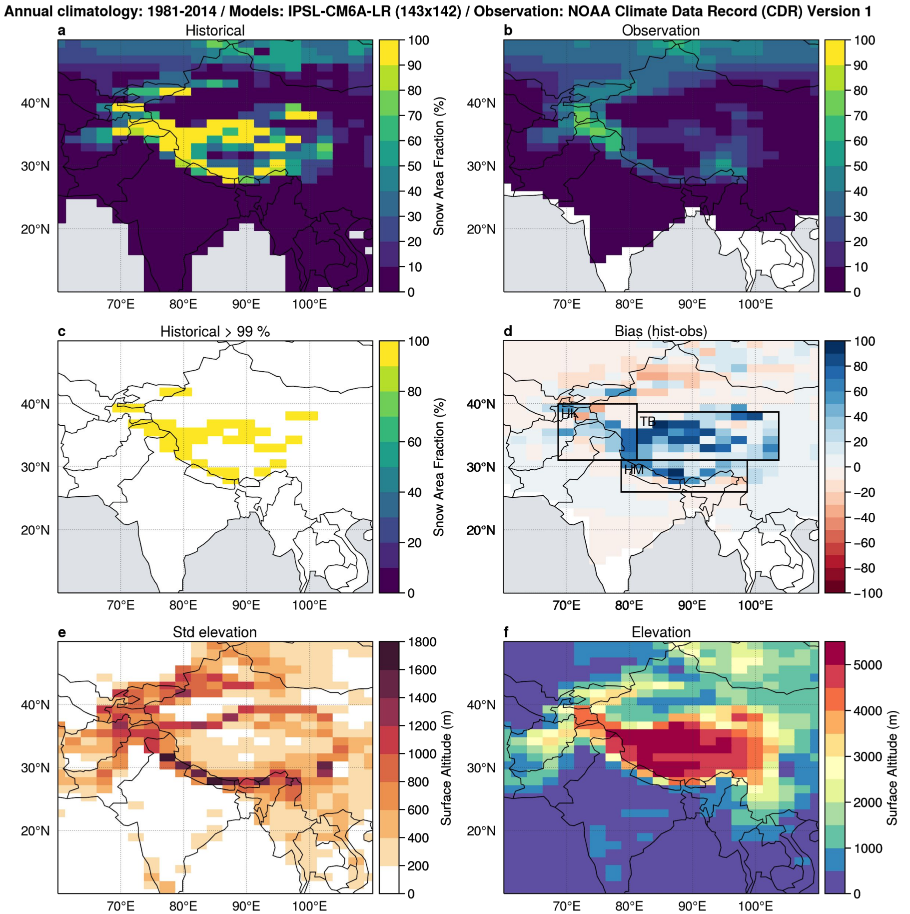

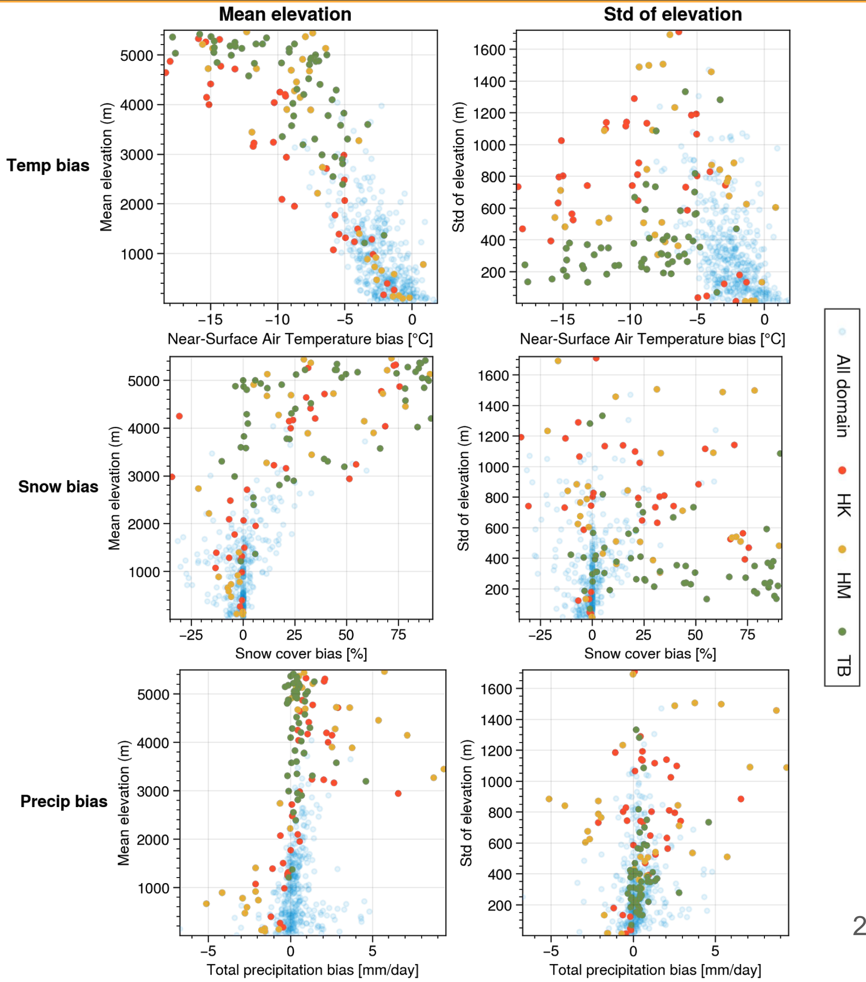

Comparaison de la topographie

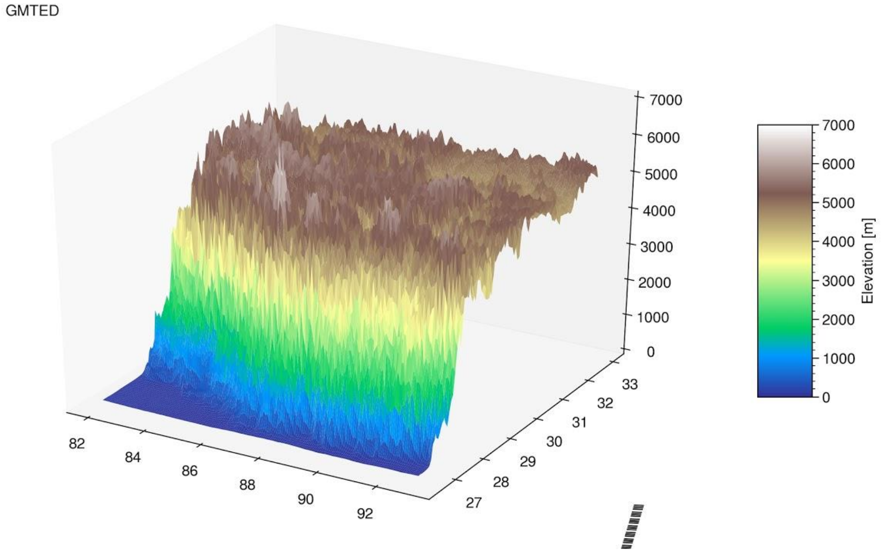

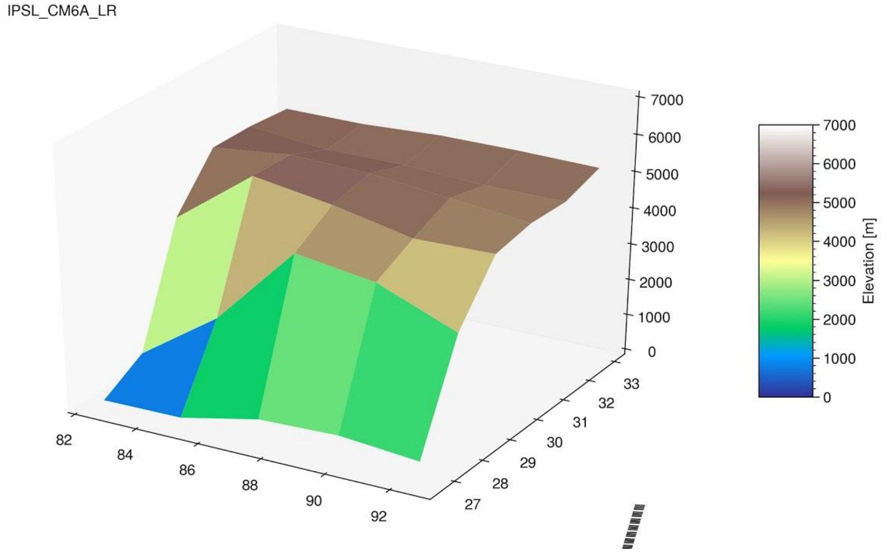

GMTED2010 à 0.0625° (~6km) de resolution

IPSL-CMA6-LR (~150x250km)

Couverture de neige

1999-2012 climatologies / Observations : MEaSUREs* (25 km de résolution)
Nearest neighbor regrid towards GMTED2010 grid (6km)

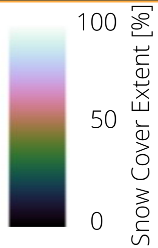

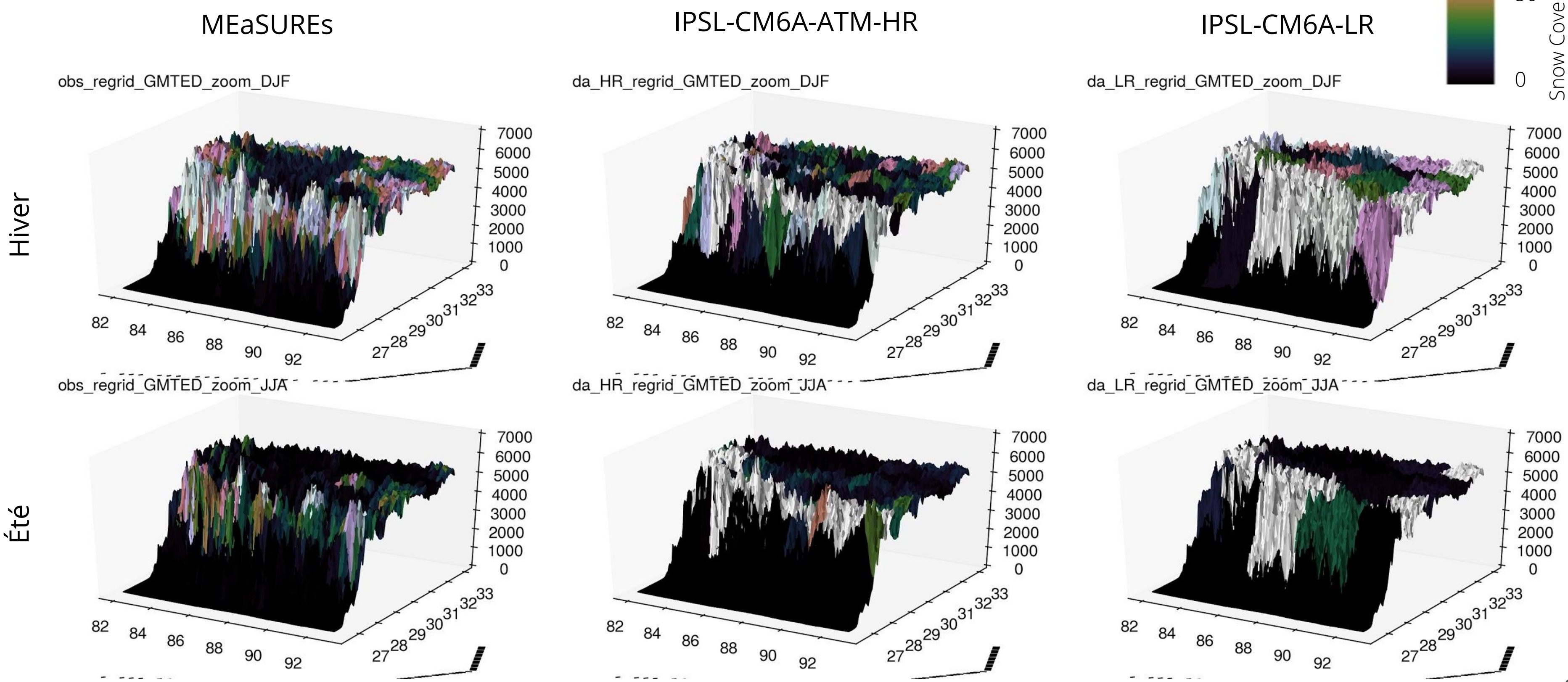

*Notebook comparaison MEaSUREs / NOAA CDR : Snow cover-MEaSUREs.ipynb + IPSL-CMA6-LR HighResMIP vs CMIP: snc_bias_HighResMIP_comparison_LR.ipynb

Paramétrisation sous-maille de la topographie

Paramétrisation sous-maille de la topographie

Problem with subgrid parameterization?

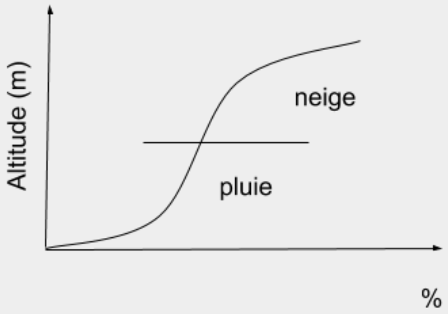

Wrong phase distribution / surface energy budget over complex terrain?

→ Walland and Simmons, 1996: SUB-GRID-SCALE TOPOGRAPHY AND THE SIMULATION OF NORTHERN HEMISPHERE SNOW COVER

→ Younas et al., 2017: A strategy to represent impacts of subgrid-scale topography on snow evolution in the Canadian Land Surface Scheme

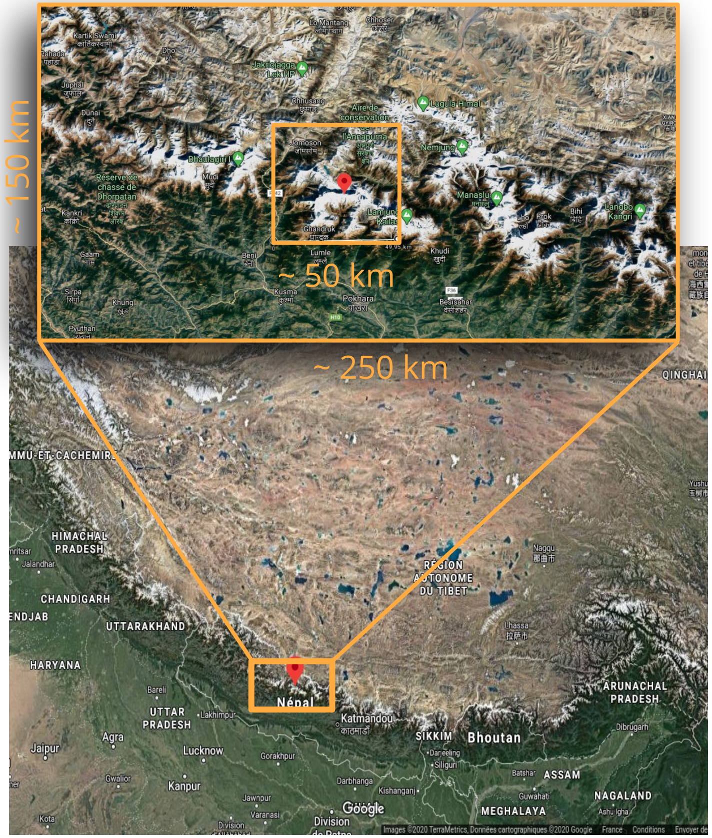

Walland and Simmons, 1996: Melbourne University GCM

Not computationally efficient to explicitly represent the height distribution on a fine scale

→ use a measure of variability of height within each grid-square together with some statistical distribution theory to approximate the distribution

~~Normal distribution?~~ include the skewness and kurtosis of the distribution

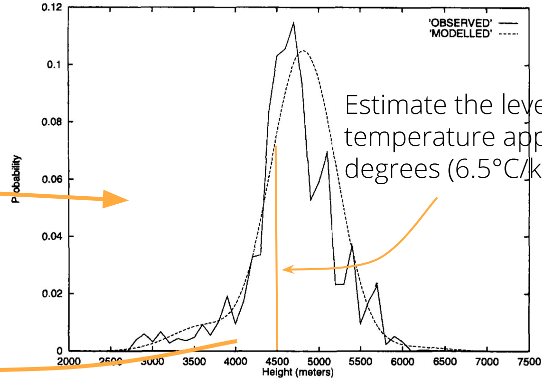

Estimate the level at which the temperature approaches zero degrees (6.5°C/km)

Figure 1. Observed and modelled distributions of height within a (5·6° × 3·3°)grid-box over the Himalayan plateau (95·6°E, 34·7°N)

Walland and Simmons (1996)

Approximation of the percentage of heights that fall below a certain level (Abramowitz and Stegun, 1965)

$$P(x) = P_{\text{nor}}(x) - \left[\frac{\gamma_3}{6} Z^{(2)}(x)\right] + \left[\frac{\gamma_4}{24} Z^{(3)}(x) + \frac{\gamma_3^2}{72} Z^{(6)}(x)\right] + \cdots$$

ablating	non-ablating

ablating:

$$T_{a_{\text{ln}}} = \frac{T_{a_{\text{mean}}} - fr_{\text{sn}} \times T_{a_{\text{sn}}}}{1{\cdot}0 - fr_{\text{sn}}}$$

$$q_{\text{sn}} = \frac{q_{sat_{\text{sn}}}}{q_{sat_{\text{mean}}}} \times q_{\text{mean}}$$

$$\frac{\partial w_g}{\partial t} = P_r - E + \text{melt}$$

$$c_p d_{\text{sn}} \frac{\partial T_s}{\partial t} = Q_s + Q_l + Q_h + Q_e + Q_m \equiv Q_{\text{tot}}$$

non-ablating:

$$T_{a_{\text{sn}}} = T_{a_{\text{mean}}} - \Delta T$$

$$q_{\text{ln}} = \frac{q_{\text{mean}} - fr_{\text{sn}} \times q_{\text{sn}}}{1{\cdot}0 - fr_{\text{sn}}}$$

$$\frac{\partial d_{\text{sn}}}{\partial t} = P_{\text{sn}} - E - \text{melt}$$

$$c_p d_{\text{sn}} \frac{\partial T_s}{\partial t} = Q_s + Q_l + Q_h + Q_e + Q_m \equiv Q_{\text{tot}}$$

New mean weighted average temperature is computed!

Younas et al., 2017: Canadian Land Surface Scheme (CLASS)

- elevation bands at 100 m intervals to capture air temperature lapse rates (6.4 °C/km)
- five slope angles on four aspects to resolve solar radiation impacts on the evolution of snow depth and SWE

Then results for snow depth and SWE averaged either over all ten elevation bands

→ elevation has more influence than slope and aspect angles when comparing spatial averages.

→ representing snowpacks using only mean (model grid cell) topographic characteristics masks the non-linear effects elevation, slope and aspect introduce in their evolution through time

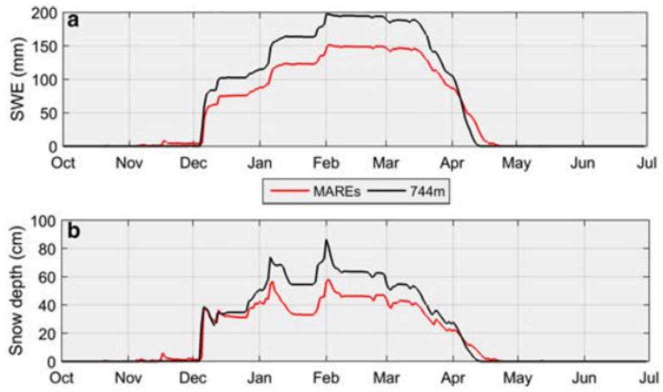

Fig. 4. Elevational dependence of average daily (a) SWE and (b) snow depth, comparing simulated CLASS results for the mean elevation (744 m) with the mean of all remaining elevations (MAREs), from 1 July 2008 to 30 June 2009.

Younas et al. (2017)

→ 26% peak SWE differences
(elevation dominates the control of peak SWE values)

Roesch et al., 2001: Include STD in the SWE/SCF relationship (ECHAM4)

- distinguish between the following three terrains: (1) non-forested areas, (2) mountainous regions and (3) forests

$$f_s = 0.95 \cdot tanh(100 \cdot S_n)\sqrt{\frac{1000 \cdot S_n}{1000 \cdot S_n + \epsilon + 0.15\sigma_z}}, \quad (7)$$

Sn is the water equivalent

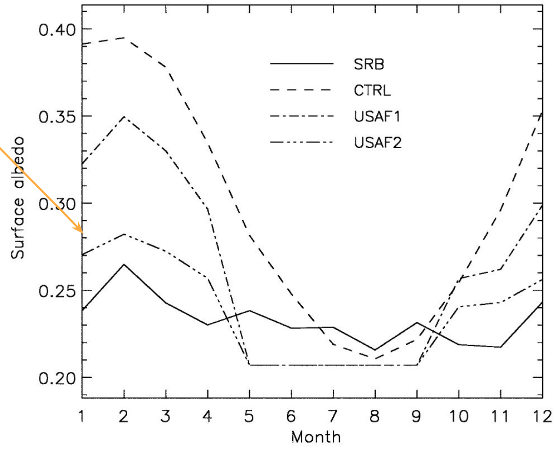

Fig. 4 Monthly mean surface albedos for the Himalayan region. *SRB*: remotely sensed surface albedo of the SRB Project (1984–1990); *CTRL*: simulation of the current climate with ECHAM4/T42; *USAF1* and *USAF2*: modified albedos based on the USAF snow depth climatology and SCFs determined with Eqs. 2 and 7, respectively

Roesch et al. (2001)

- Already coded by Gerhard and Martin (code_martin_neige_aerosol_2014) + aerosols

  but not implemented in the official code

- Actual formula in ORCHIDEE:

$$frac_{\text{snow,veg}} = \tanh\frac{50 \cdot d_{\text{snow}}}{0.025 \cdot \rho_{\text{snow}}}$$

Swenson & Lawrence, 2012: New SWE/SCF relationship (CLM4)

$$F = \tanh\left(\frac{d}{2.5 z_{0g} (\rho_{snow}/\rho_{new})^m}\right)$$

$$F = 1 - \left[\frac{1}{\pi}\operatorname{acos}\left(2\frac{W}{W_{\max}} - 1\right)\right]^{N_{melt}}$$

$$N_{melt} = \frac{200}{\sigma_{topo}}$$

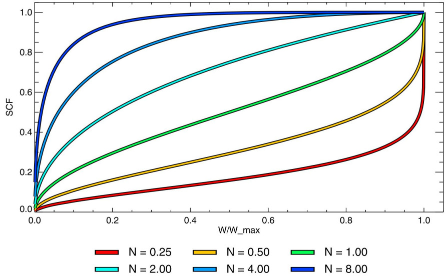

Figure 9. Depletion curves defined by equation (4) for different values of the shape parameter N_{melt}. The x axis is snow depth in meters, and the y axis is SCF.

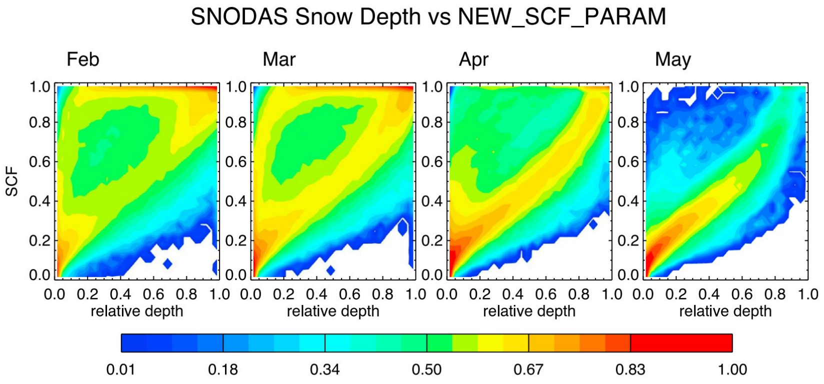

Figure 10. Histograms of predicted SCF, derived from SNODAS snow depth data and equations (4) and (5).

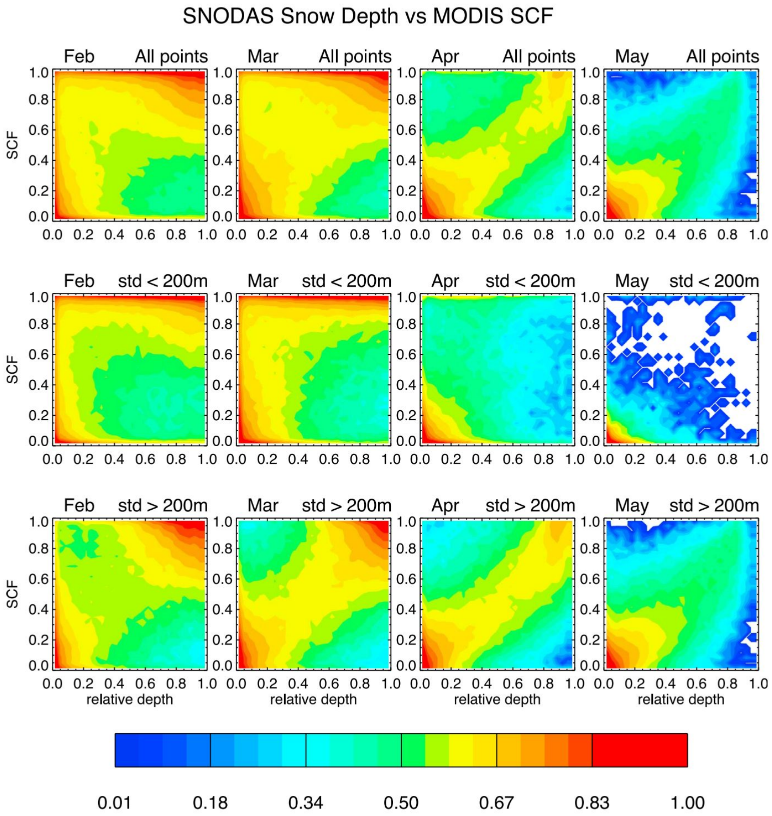

Figure 8. Histograms of relative depth and SCF based on SNODAS snow depth data and MODIS SCF data. Contours represent logarithm of number of points. (top) Histograms based on all points. (middle) Histogram based on points having low topographic variability ($\sigma \leq 200$ m). (bottom) Histogram based on points having high topographic variability ($\sigma \geq 200$ m).

Éléments de code

Albedo

- [https://orchidas.lsce.ipsl.fr/dev/**albedo**/](https://orchidas.lsce.ipsl.fr/dev/albedo/)

Code Orchidée

- http://forge.ipsl.jussieu.fr/orchidee/browser/branches/ORCHIDEE_2_2/ORCHIDEE/src_sechiba/**explicitsnow**.f90
- http://forge.ipsl.jussieu.fr/orchidee/browser/branches/ORCHIDEE_2_2/ORCHIDEE/src_sechiba/**condveg**.f90
- http://forge.ipsl.jussieu.fr/orchidee/browser/branches/ORCHIDEE_2_2/ORCHIDEE/src_sechiba/**enerbil**.f90

"An independent hydrological budget is calculated for each soil tile, to prevent forests from exhausting all soil moisture. In contrast, only one energy budget (and snow budget) is calculated for the whole grid cell. "

Boucher et al. (2020)

Code LMDZ topography

- http://trac.lmd.jussieu.fr/LMDZ/browser/LMDZ6/trunk/libf/phylmd/**grid_noro_m**.F90

```
REAL, INTENT(OUT) :: zmea(:,:)      !--- MEAN OROGRAPHY          (imar+1,jmar)
REAL, INTENT(OUT) :: zstd(:,:)      !--- STANDARD DEVIATION      (imar+1,jmar)
REAL, INTENT(OUT) :: zsig(:,:)      !--- SLOPE                   (imar+1,jmar)
REAL, INTENT(OUT) :: zgam(:,:)      !--- ANISOTROPY              (imar+1,jmar)
REAL, INTENT(OUT) :: zthe(:,:)      !--- SMALL AXIS ORIENTATION  (imar+1,jmar)
REAL, INTENT(OUT) :: zpic(:,:)      !--- MAXIMUM ALTITITUDE      (imar+1,jmar)
REAL, INTENT(OUT) :: zval(:,:)      !--- MINIMUM ALTITITUDE      (imar+1,jmar)
```

```
!=== FILTERS TO SMOOTH OUT FIELDS FOR INPUT INTO SSO SCHEME.
!--- FIRST FILTER, MOVING AVERAGE OVER 9 POINTS.
!-------------------------------------------------------------------------------
  zphi(:,:)=zmea(:,:)                                ! GK211005 (CG) UNSMOOTHED TOPO

  CALL MVA9(zmea);  CALL MVA9(zstd);  CALL MVA9(zpic);  CALL MVA9(zval)
  CALL MVA9(zxtzx); CALL MVA9(zxtzy); CALL MVA9(zytzy)
```

Autres prospectives

Autres prospectives

Objectif final : essayer de détecter les changements futur en HMA et les attribuer à des changements dynamique / thermodynamique et/ou aux changements anthropiques (CO2, aérosols, etc.)

- Introduction de la nouvelle paramétrisation sous-maille (en cas de succès) dans le modèle afin de faire des simulations plus précises et mieux représenter les changements de la cryosphère
- Papier multimodèle (CMIP6) en incluant les projections
- Simulation zoomée (voire guidée) pour une validation avec les observations GLACIOCLIM et envisager des simulations longues (1850-2100)
- Etudier les expériences DAMIP déjà a disposition pour étudier l'impact des forçages
- Appliquer la méthode des analogues décrite dans Deser et al. (2016) afin de détecter des changements dans la région des HMA et de les attribuer à des changements dynamiques ou thermodynamiques de l'atmosphère

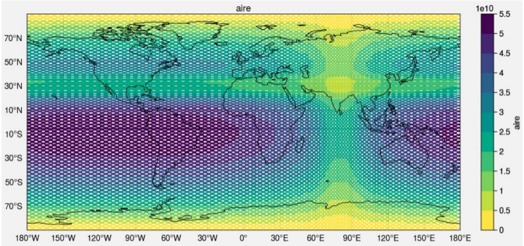

Exemple de grille zoomée

Conclusions

Conclusions sur le déroulement de la thèse

Thèse

- **Début de première année** : formations, biblio, prise en main des outils
- **Milieu de première année** : Analyse des biais + essaie de simulations
  ➝ Biais plus important dans LMDZ CMIP6 (couplé) que CMIP5 sur les HMA (lien possible avec la troposphère, la topographie, les précipitations et d'autres variables non étudiées : albédo, couverture nuageuse, aérosols, couche limite, bilan énergétique de surface)
- **Fin de première année** : Analyse multimodèle CMIP6 + paramétrisation de la couverture de neige liée à la topographie sous-maille dans LMDZ + autres

Encadrement

- Encadrants, labo, Grenoble top ➝ toujours aussi motivé pour la suite !

Perso

- Pas mal investi dans les outils émergents d'analyses (Python, Jupyter, xarray, dask, intake, proplot, xESMF, etc.)
  - MC-Toolkit à l'IGE / Échange avec Guillaume Levasseur pour mettre en place sur CICLAD un catalogue Intake + Dask (parallélisation) + environnement Pangeo
  - Tout mon projet est sur Github (+ liens sur les figures) + présentations sur mon site internet

Bonus

- Projet de chaîne Youtube sur la vulgarisation autours du climat (Sciences et Climat)
- Quelques photos de randonnées

Conclusions

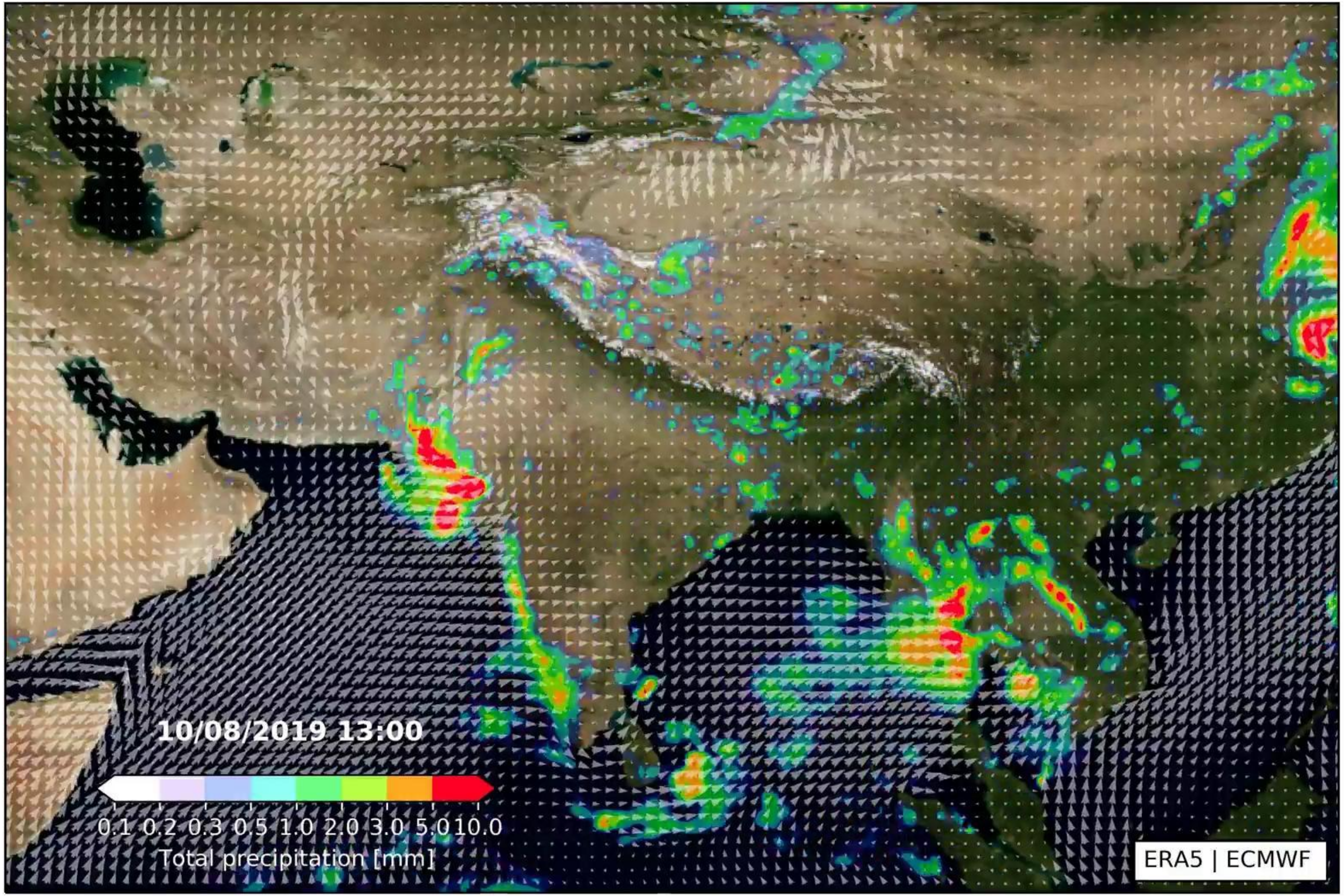

Bibliographie

References

Abramowitz, M., & Irene, S. (1964). Handbook of Mathematical Functions, pp. 931-995. Retrieved from http://people.math.sfu.ca/~cbm/aands/abramowitz_and_stegun.pdf

Bookhagen, B., & Burbank, D. W. (2010). Toward a complete Himalayan hydrological budget: Spatiotemporal distribution of snowmelt and rainfall and their impact on river discharge. Journal of Geophysical Research: Earth Surface, 115(3), 1–25. https://doi.org/10.1029/2009JF001426

Boos, W. R., & Hurley, J. V. (2013). Thermodynamic bias in the multimodel mean boreal summer monsoon. Journal of Climate, 26(7), 2279–2287. https://doi.org/10.1175/JCLI-D-12-00493.1

Boucher, O., Servonnat, J., Albright, A. L., Aumont, O., Balkanski, Y., Bastrikov, V., ... Vuichard, N. (2020). Presentation and Evaluation of the IPSL-CM6A-LR Climate Model. Journal of Advances in Modeling Earth Systems, 12(7), 1–52. https://doi.org/10.1029/2019MS002010

Chen, X., Liu, Y., & Wu, G. (2017). Understanding the surface temperature cold bias in CMIP5 AGCMs over the Tibetan Plateau. Advances in Atmospheric Sciences, 34(12), 1447–1460. https://doi.org/10.1007/s00376-017-6326-9

Cheruy, F., Ducharne, A., Hourdin, F., Musat, I., Vignon, E., Gastineau, G., ... Zhao, Y. (2020). Improved near surface continental climate in IPSL-CM6A-LR by combined evolutions of atmospheric and land surface physics. Journal of Advances in Modeling Earth Systems, 2019MS002005, submitted. https://doi.org/10.1029/2019MS002005

Deser, C., Terray, L., & Phillips, A. S. (2016). Forced and internal components of winter air temperature trends over North America during the past 50 years: Mechanisms and implications. Journal of Climate, 29(6), 2237–2258. https://doi.org/10.1175/JCLI-D-15-0304.1

References

Gu, H., Wang, G., Yu, Z., & Mei, R. (2012). Assessing future climate changes and extreme indicators in east and south Asia using the RegCM4 regional climate model. Climatic Change, 114(2), 301–317. https://doi.org/10.1007/s10584-012-0411-y

Immerzeel, W. W., Wanders, N., Lutz, A. F., Shea, J. M., & Bierkens, M. F. P. (2015). Reconciling high-altitude precipitation in the upper Indus basin with glacier mass balances and runoff. Hydrology and Earth System Sciences, 19(11), 4673–4687. https://doi.org/10.5194/hess-19-4673-2015

Lee, D. K., & Suh, M. S. (2000). Ten-year east Asian summer monsoon simulation using a regional climate model (RegCM2). Journal of Geophysical Research Atmospheres, 105(D24), 29565–29577. https://doi.org/10.1029/2000JD900438

Li, C., Su, F., Yang, D., Tong, K., Meng, F., & Kan, B. (2018). Spatiotemporal variation of snow cover over the Tibetan Plateau based on MODIS snow product, 2001-2014. International Journal of Climatology, 38(2), 708–728. https://doi.org/10.1002/joc.5204

Mao, J., & Robock, A. (1998). Surface Air Temperature Simulations by AMIP General Circulation Models: Volcanic and ENSO Signals and Systematic Errors. Journal of Climate, 11(7), 1538–1552. https://doi.org/10.1175/1520-0442(1998)011<1538:SATSBA>2.0.CO;2

Orsolini, Y., Wegmann, M., Dutra, E., Liu, B., Balsamo, G., Yang, K., … Arduini, G. (2019). Evaluation of snow depth and snow cover over the Tibetan Plateau in global reanalyses using in situ and satellite remote sensing observations. The Cryosphere, 13(8), 2221–2239. https://doi.org/10.5194/tc-13-2221-2019

Palazzi, E., von Hardenberg, J., & Provenzale, A. (2013). Precipitation in the Hindu-Kush Karakoram Himalaya: Observations and future scenarios. Journal of Geophysical Research: Atmospheres, 118(1), 85–100. https://doi.org/10.1029/2012JD018697

References

Roesch, A., Wild, M., Gilgen, H., & Ohmura, A. (2001). A new snow cover fraction parametrization for the ECHAM4 GCM. Climate Dynamics, 17(12), 933–946. https://doi.org/10.1007/s003820100153

Serafin, S., Rotach, M. W., Arpagaus, M., Colfescu, I., Cuxart, J., De Wekker, S. F. J., ... Zardi, D. (2020). Multi-scale transport and exchange processes in the atmosphere over mountains. In Multi-scale transport and exchange processes in the atmosphere over mountains. https://doi.org/10.15203/99106-003-1

Sharma, E., Molden, D., Rahman, A., Khatiwada, Y. R., Zhang, L., Singh, S. P., ... Wester, P. (2019). Introduction to the Hindu Kush Himalaya Assessment. In The Hindu Kush Himalaya Assessment (pp. 1–16). https://doi.org/10.1007/978-3-319-92288-1_1

Smith, T., & Bookhagen, B. (2018). Changes in seasonal snow water equivalent distribution in High Mountain Asia (1987 to 2009). *Science Advances*, *4*(1), e1701550. https://doi.org/10.1126/sciadv.1701550

Su, F., Duan, X., Chen, D., Hao, Z., & Cuo, L. (2013). Evaluation of the Global Climate Models in the CMIP5 over the Tibetan Plateau. Journal of Climate, 26(10), 3187–3208. https://doi.org/10.1175/JCLI-D-12-00321.1

Swenson, S. C., & Lawrence, D. M. (2012). A new fractional snow-covered area parameterization for the Community Land Model and its effect on the surface energy balance. Journal of Geophysical Research: Atmospheres, 117(D21), n/a-n/a. https://doi.org/10.1029/2012JD018178

Usha, K. H., Nair, V. S., & Babu, S. S. (2020). Modeling of aerosol induced snow albedo feedbacks over the Himalayas and its implications on regional climate. Climate Dynamics, (0123456789). https://doi.org/10.1007/s00382-020-05222-5

References

WALLAND, D. J., & SIMMONDS, I. (1996). SUB-GRID-SCALE TOPOGRAPHY AND THE SIMULATION OF NORTHERN HEMISPHERE SNOW COVER. International Journal of Climatology, 16(9), 961–982. http://doi.wiley.com/10.1002/%28SICI%291097-0088%28199609%2916%3A9%3C961%3A%3AAID-JOC72%3E3.0.CO%3B2-R

Wang, T., Ottlé, C., Boone, A., Ciais, P., Brun, E., Morin, S., ... Peng, S. (2013). Evaluation of an improved intermediate complexity snow scheme in the ORCHIDEE land surface model. Journal of Geophysical Research: Atmospheres, 118(12), 6064–6079. https://doi.org/10.1002/jgrd.50395

Wang, X., Yang, M., Wan, G., Chen, X., & Pang, G. (2013). Qinghai-Xizang (Tibetan) Plateau climate simulation using the regional climate model RegCM3. Climate Research, 57(3), 173–186. https://doi.org/10.3354/cr01167

Yao, T., Thompson, L., Yang, W., Yu, W., Gao, Y., Guo, X., ... Joswiak, D. (2012). Different glacier status with atmospheric circulations in Tibetan Plateau and surroundings. Nature Climate Change, 2(9), 663–667. https://doi.org/10.1038/nclimate1580

Younas, W., Hay, R. W., MacDonald, M. K., Islam, S. U., & Déry, S. J. (2017). A strategy to represent impacts of subgrid-scale topography on snow evolution in the Canadian Land Surface Scheme. Annals of Glaciology, 58(75pt1), 1–10. https://doi.org/10.1017/aog.2017.29

Slides complémentaires

Near-Surface Air Temperature climatologies (CRU)

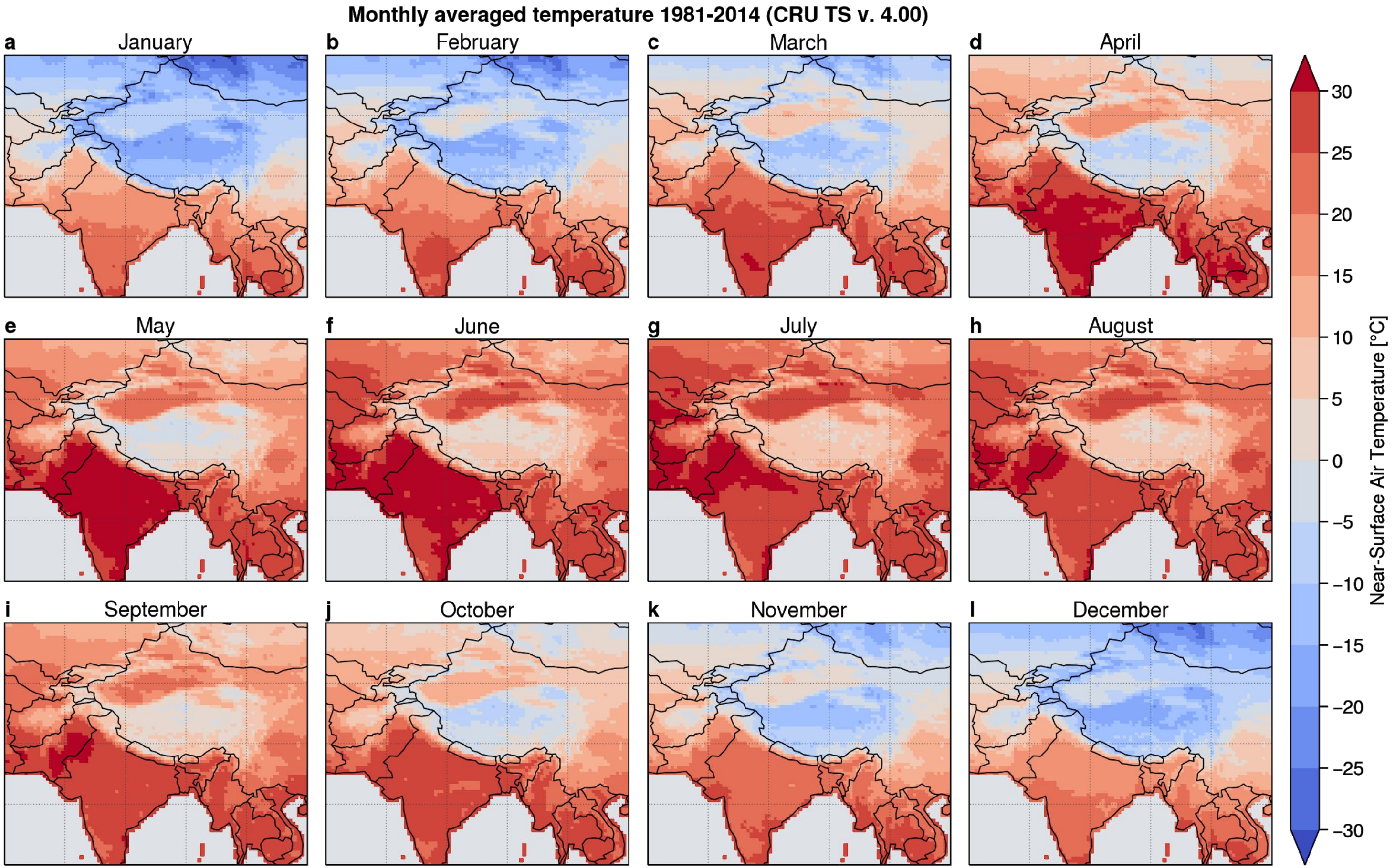

Monthly snow cover climatologies (from satellite observations)

[NOAA Climate Data Record (CDR) of Northern Hemisphere (NH) Snow Cover Extent (SCE), Version 1](#) (1981-2014)

[MODIS/Terra Snow Cover 8-Day L3 Global 0.05Deg CMG, Version 6](#) (2001-2014)

Li et al. ([2018](#)), [Fig. 2](#)

Monthly averaged snow cover 1981-2014 (NOAA Climate Data Record (CDR) Version 1)

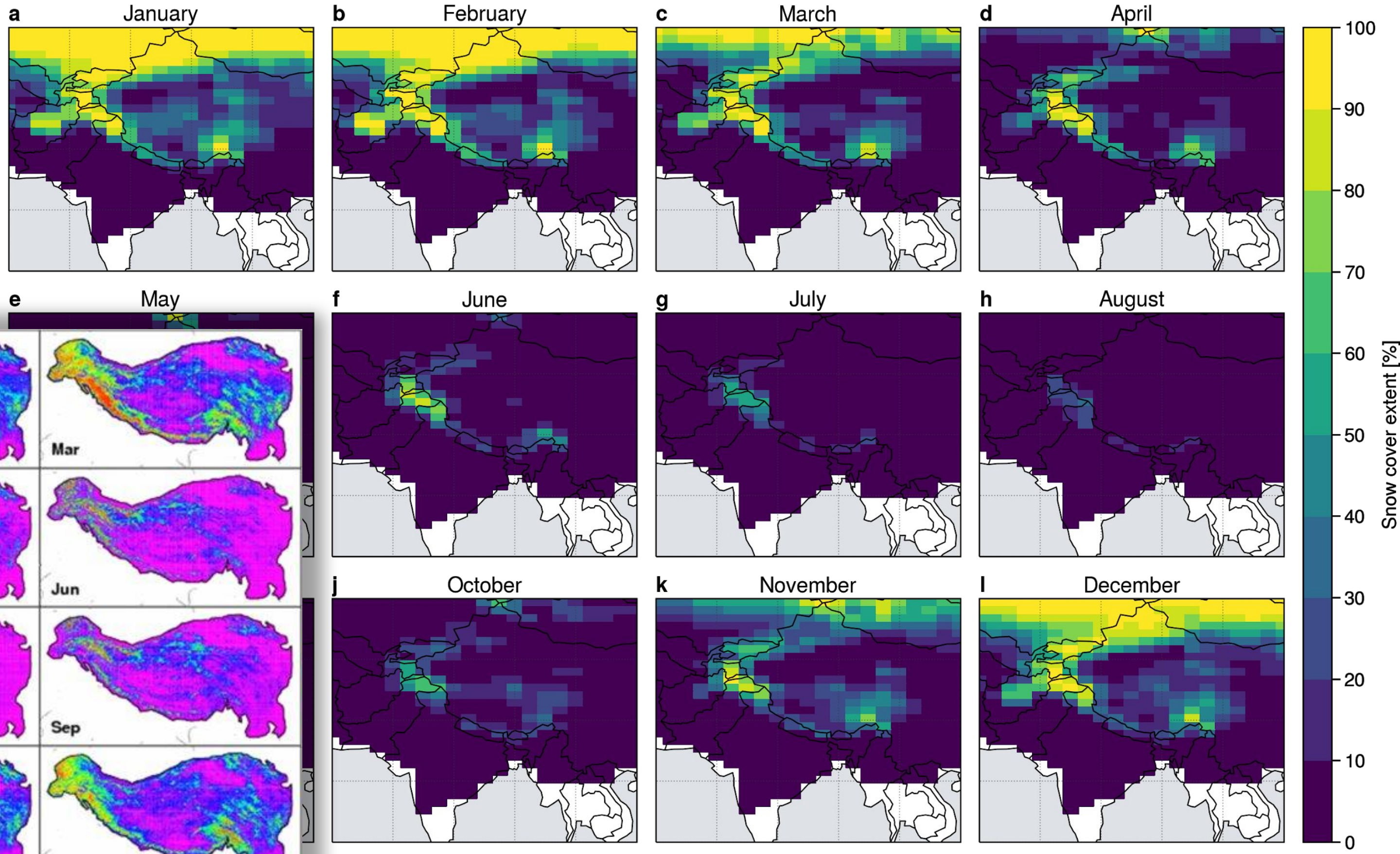

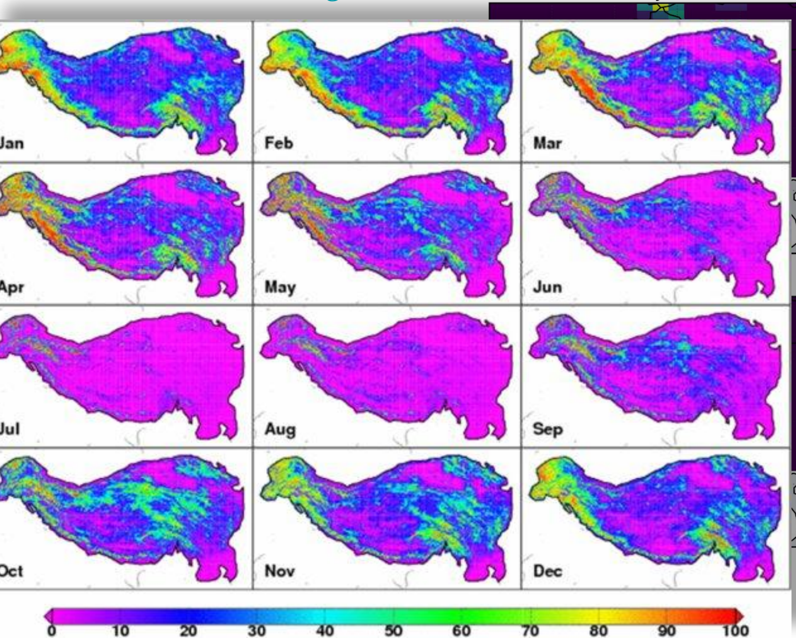

Precipitation climatologies (APHRODITE)

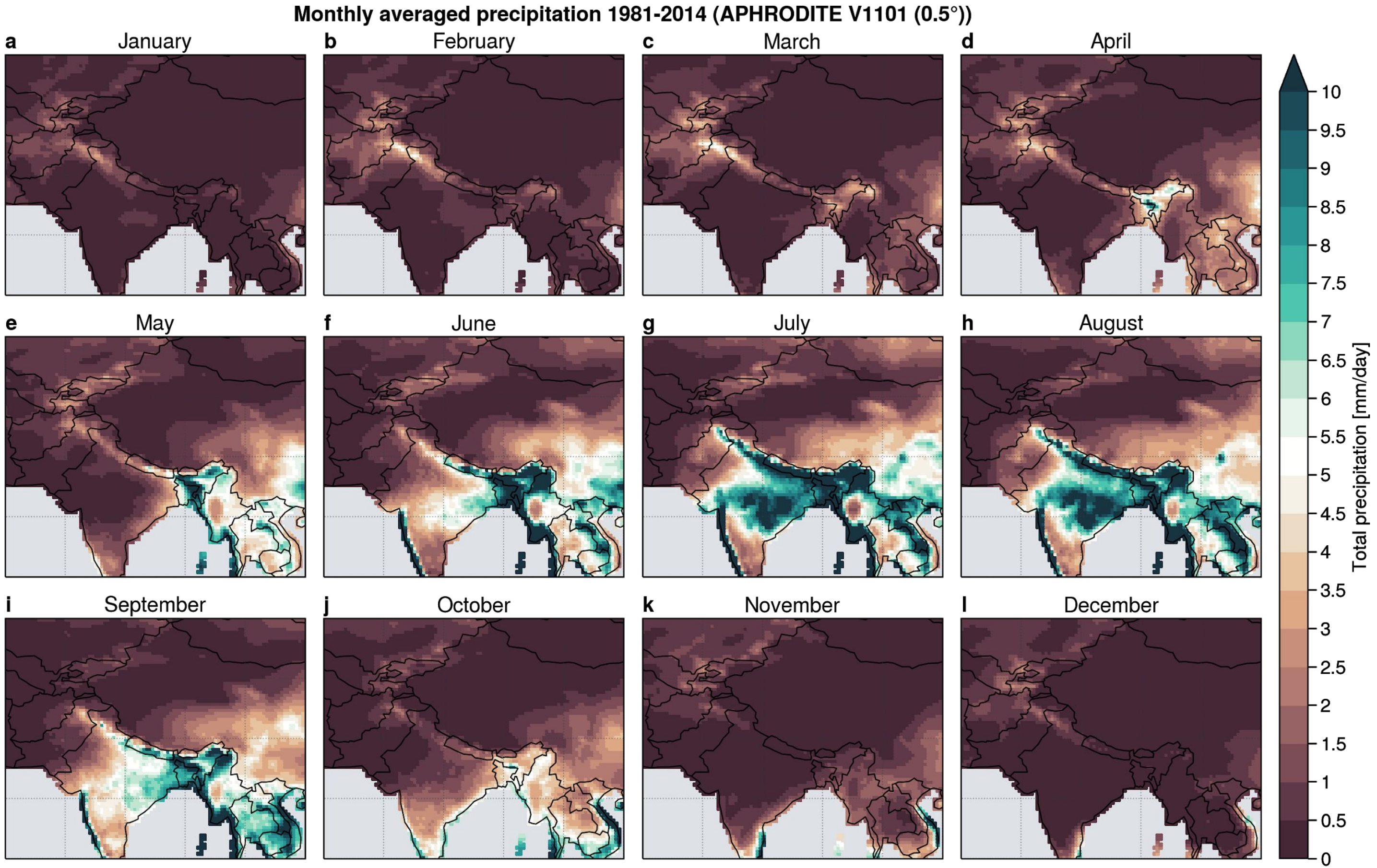

IPSL-CM6A-LR: Historical, AMIP, land-hist / IPSL-CM6A-ATM-HR bias

Total precipitation **relative** bias
(versus stations observations)

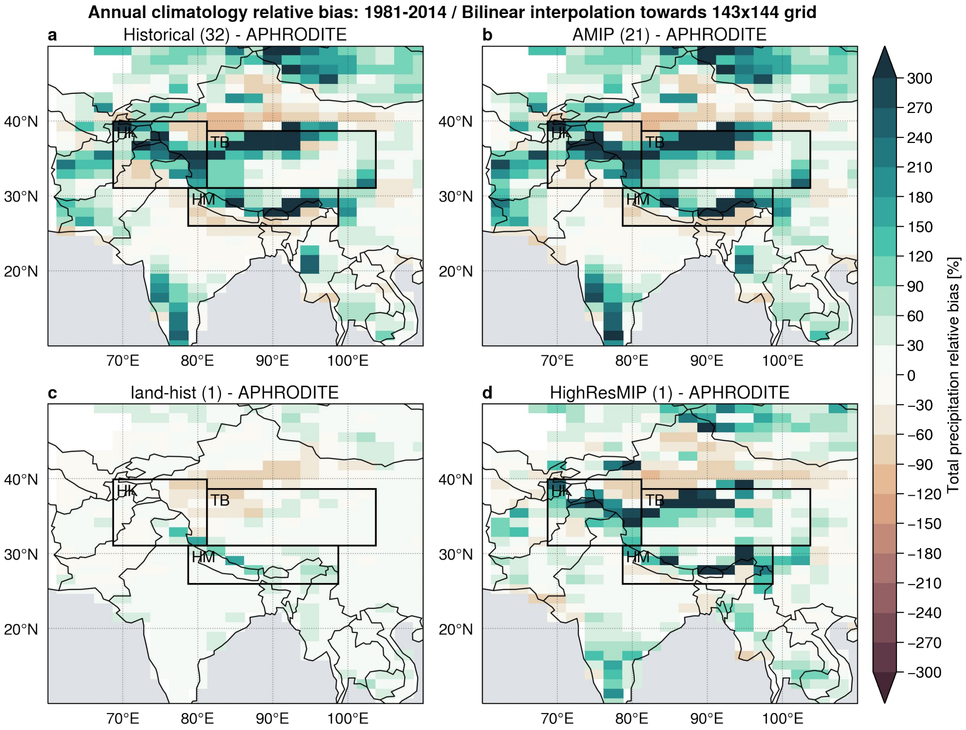

BUT… ([see ERAI](#))

All in situ stations and satellite data tends to underestimate the snow component!

- The in situ station and satellite data, as well as their combinations, have difficulties in detecting the snow component of precipitation. (Palazzi et al., [2013](#))
- An independent validation with observed river flow confirms that the water balance can indeed only be closed when the high altitude precipitation on average is more than twice as high and in extreme cases up to a factor of 10 higher than previously thought. (Immerzeel et al., [2015](#))

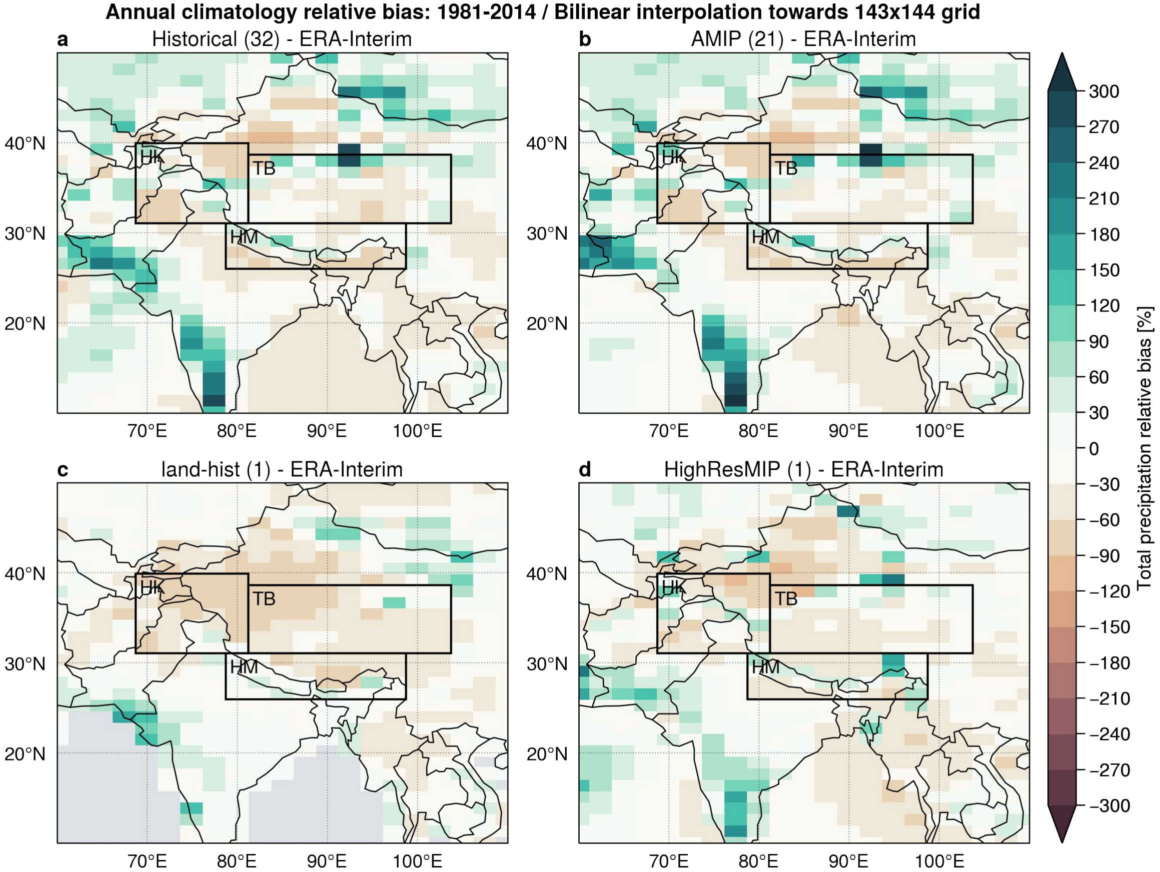

Total precipitation **relative** bias

(versus reanalysis)

BUT…

"ERA-Interim strongly overestimates precipitation compared to the other data sets, and so does EC-Earth in the HKK domain, probably owing to the fact that both ERA-Interim and EC-Earth provide total precipitation while the in situ station and satellite data, as well as their combinations, have difficulties in detecting the snow component of precipitation. The analysis of liquid-only precipitation in ERA-Interim and EC-Earth generally gives results closer to the observations." (Palazzi et al., 2013)

Back

Precipitation: annual cycles

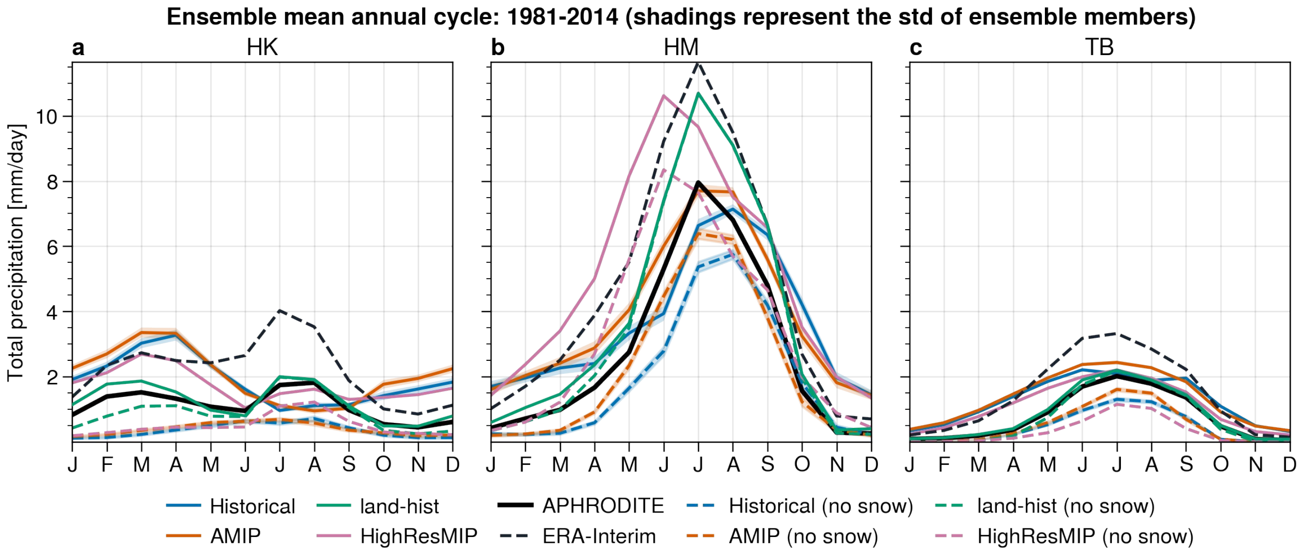

*"**ERA-Interim strongly overestimates precipitation** compared to the other data sets, and so does EC-Earth in the HKK domain, probably owing to the fact that both **ERA-Interim and EC-Earth provide total precipitation while the in situ station and satellite data, as well as their combinations, have difficulties in detecting the snow component of precipitation**. The analysis of liquid-only precipitation in ERA-Interim and EC-Earth generally gives results closer to the observations."*

(Palazzi et al., 2013)

Nudged versus not nudged

More:
https://docs.google.com/document/d/1SphVviaGEyB9KQbkgC4U2hC-qraRfaE-ojLayZcDGPU/edit?usp=sharing

Back

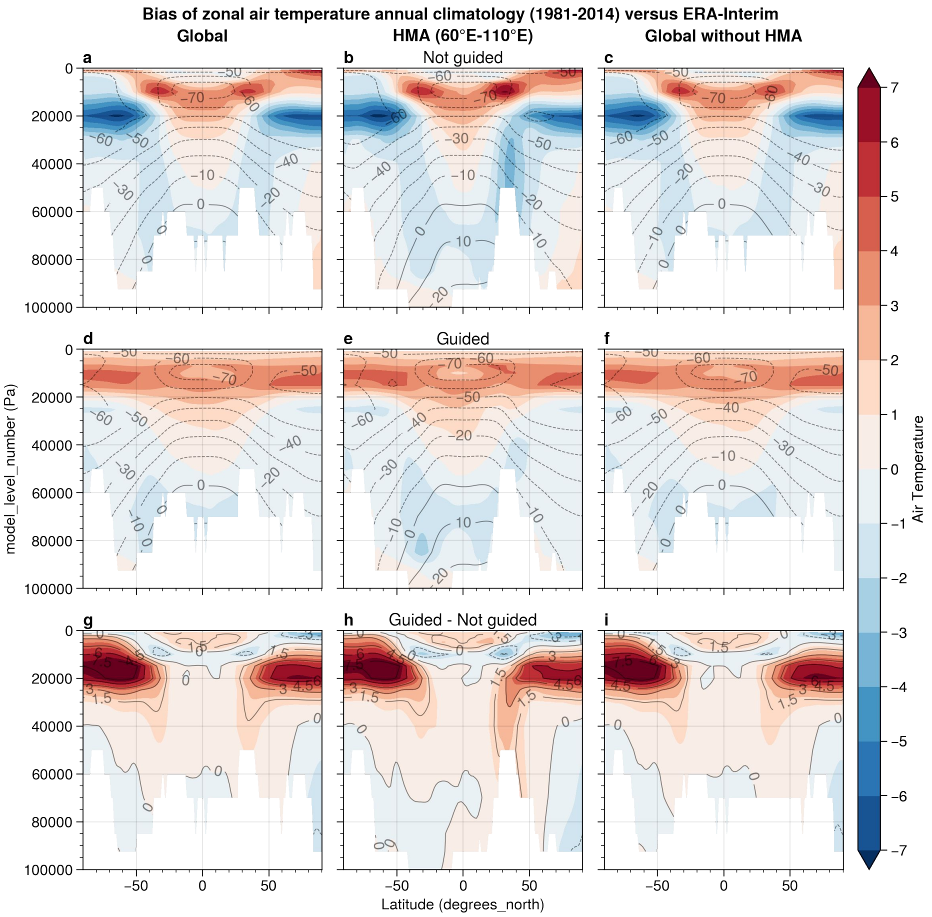

Dynamico versus HighResMIP: snow cover*

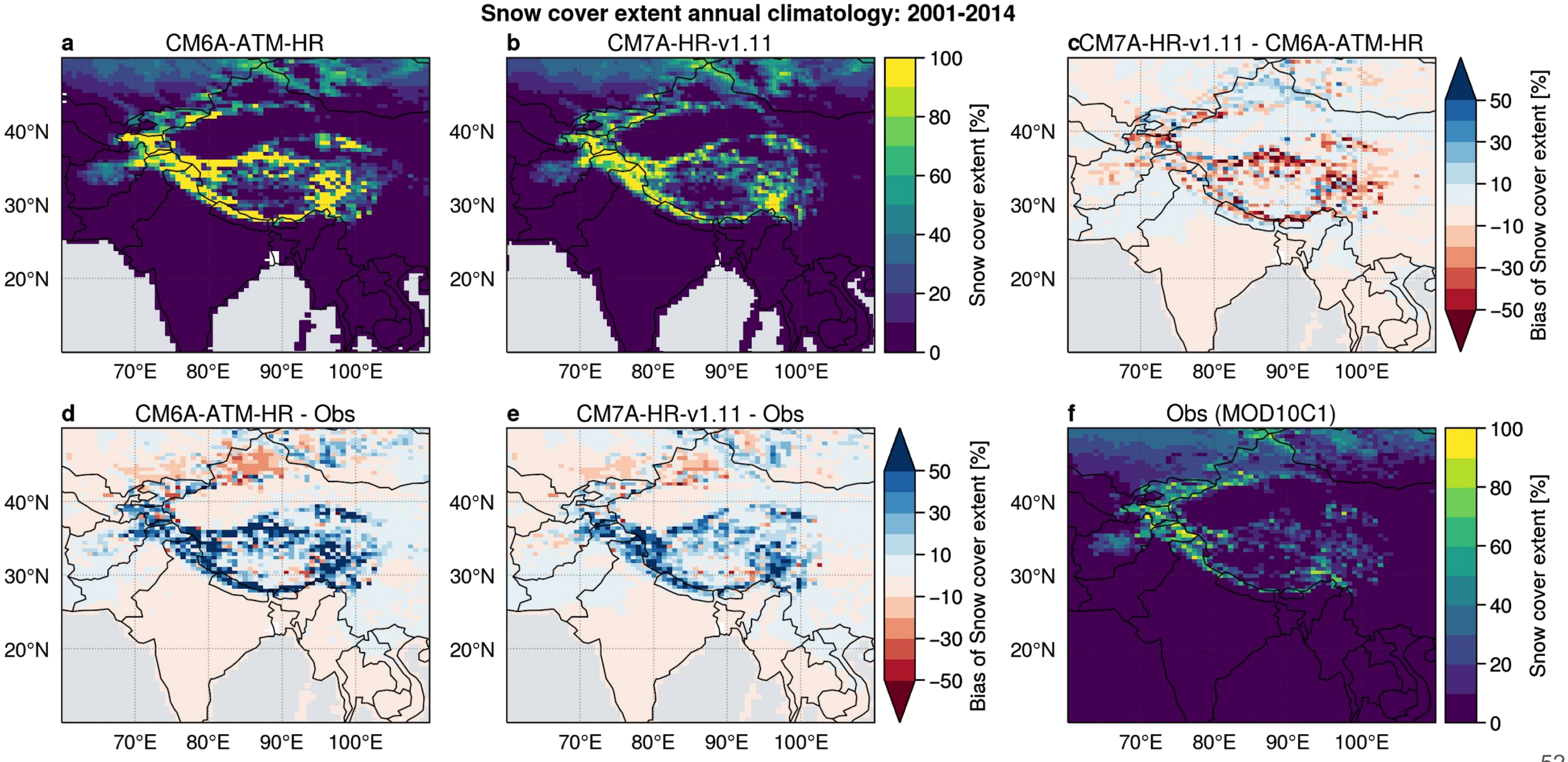

* Simulation: Sebastien FROMANG

Air Temperature of historical (r1i1p1f1)

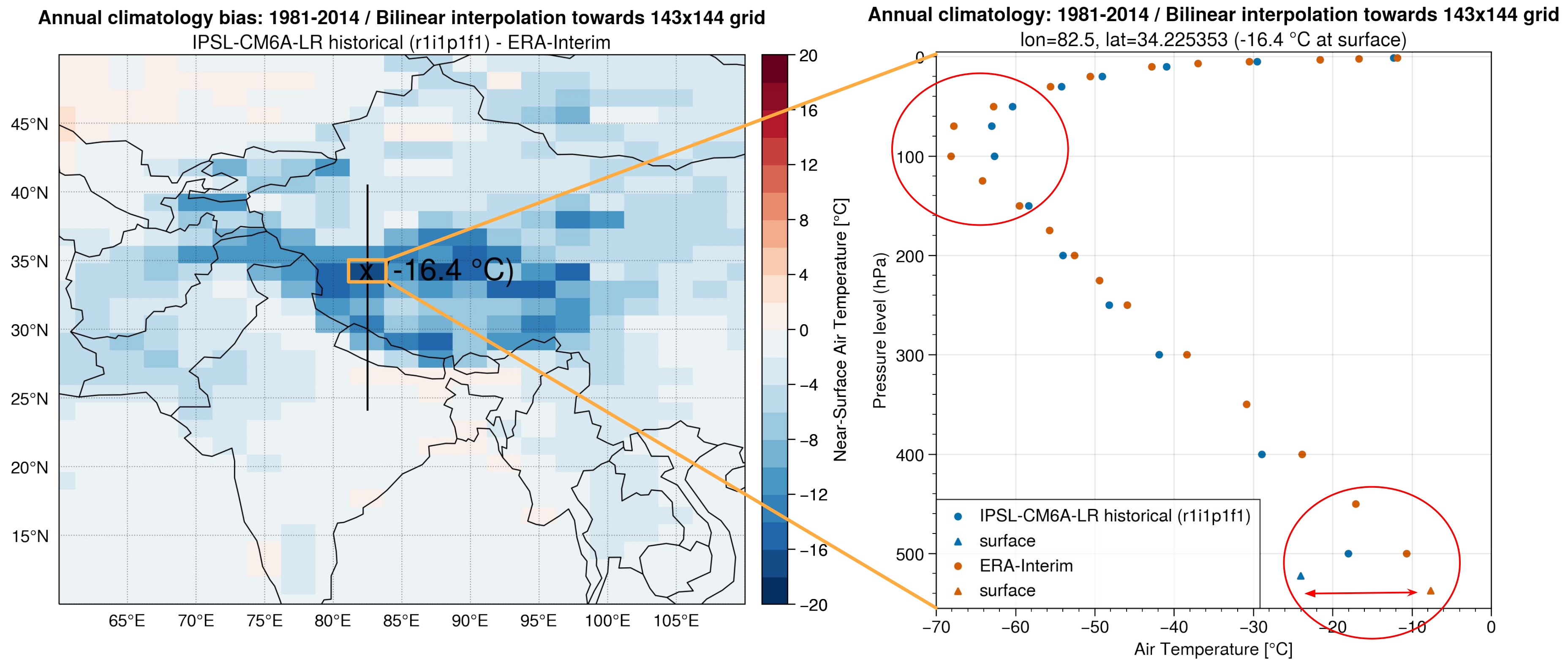

Snow evolution

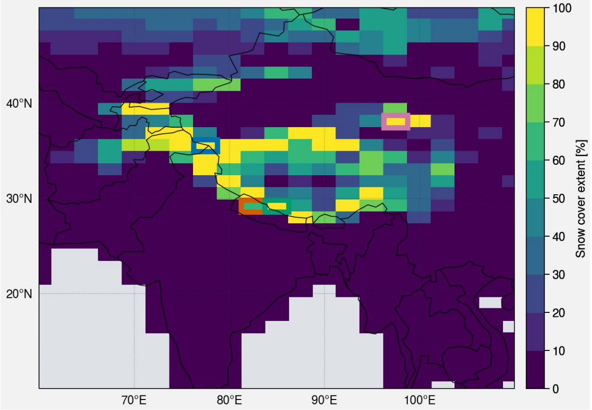

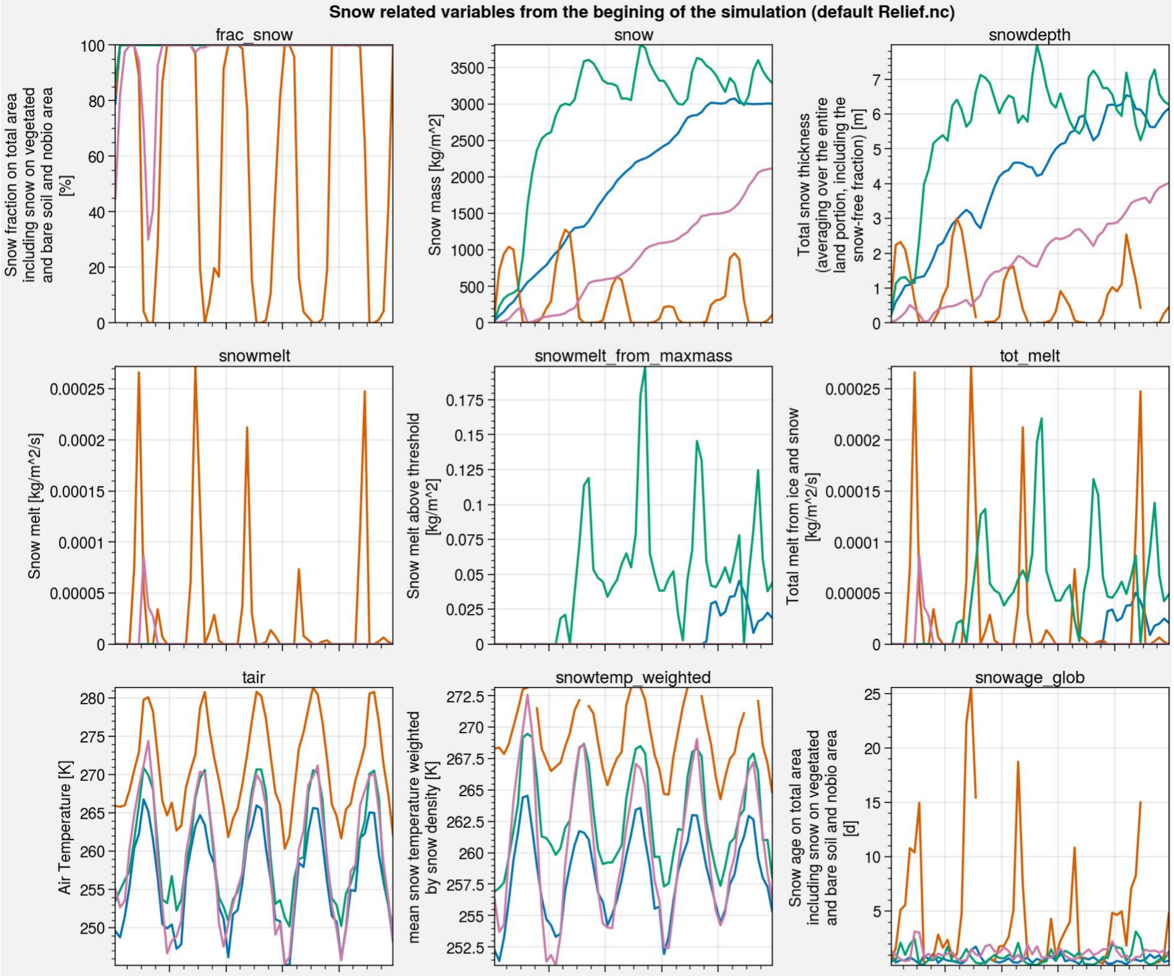

Paramétrisation sous-maille de la topographie

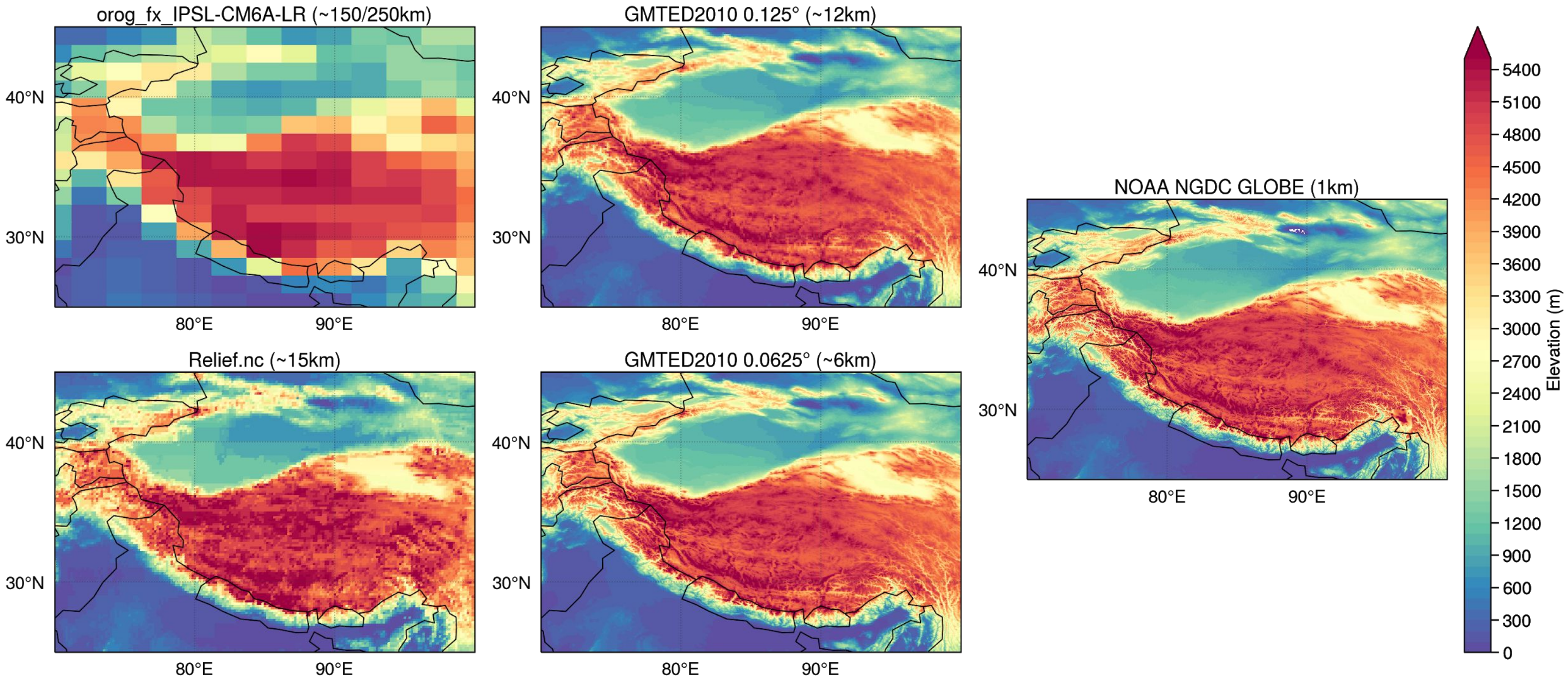

Paramétrisation sous-maille de la topographie

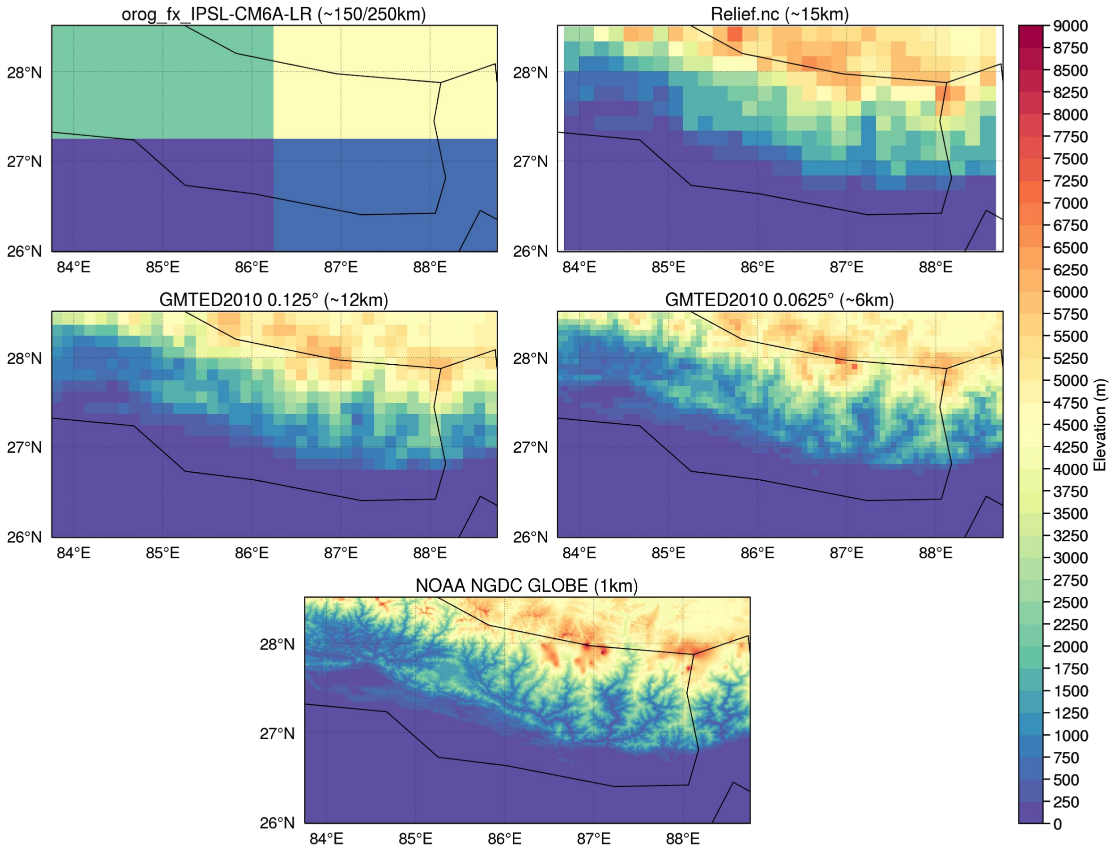

CMIP6 other models: Annual cycles

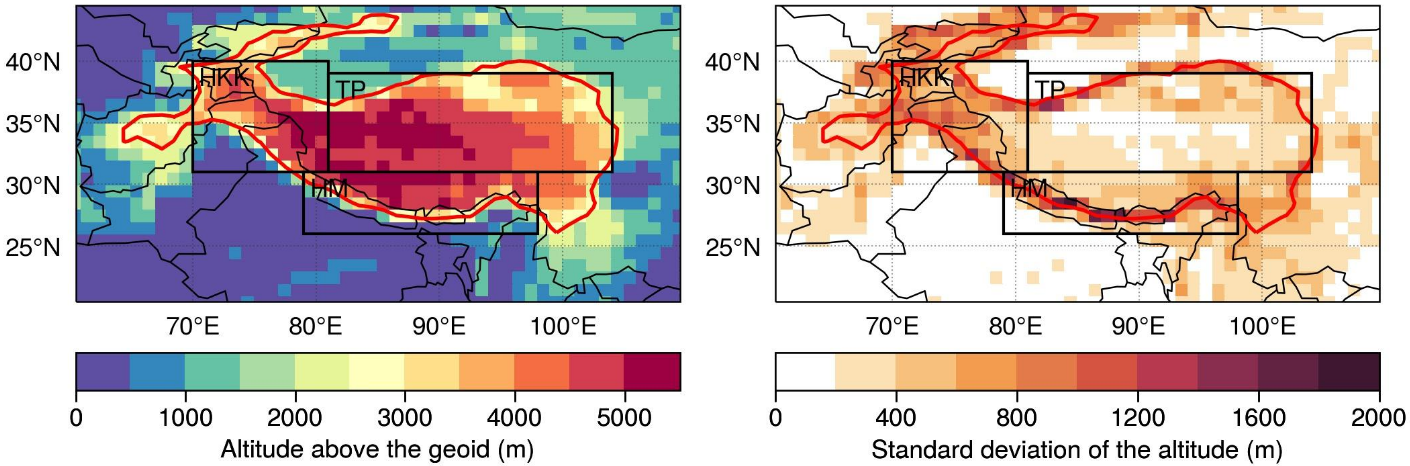

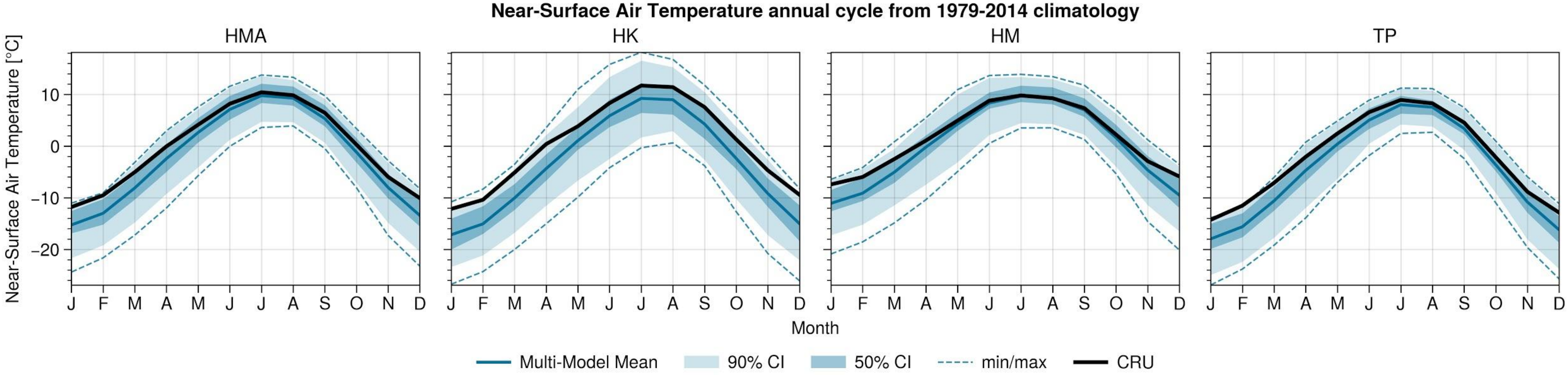

CMIP6 other models: Annual cycles

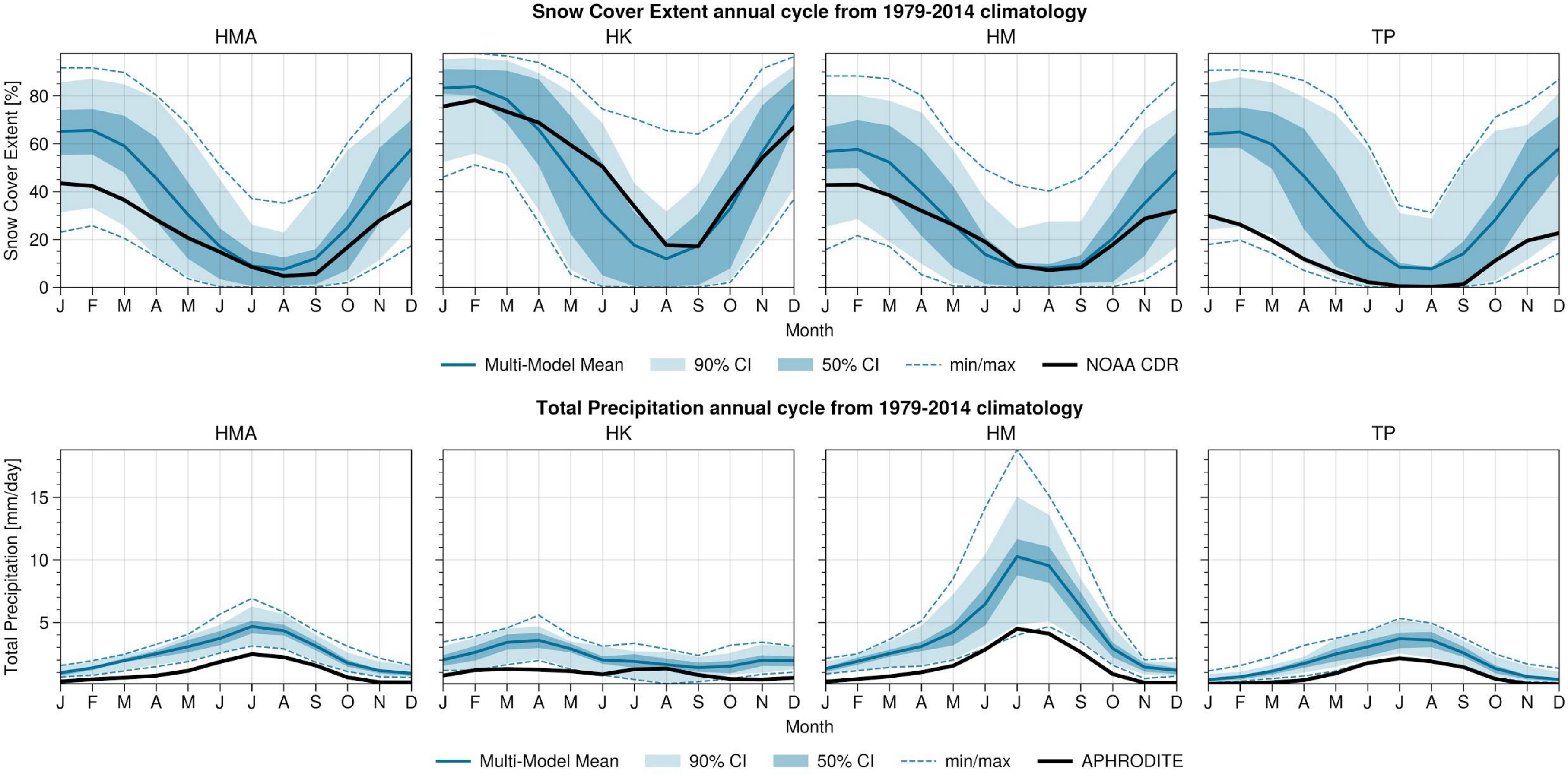

CMIP6 other models: Near-Surface Air Temperature metrics

Snow Cover

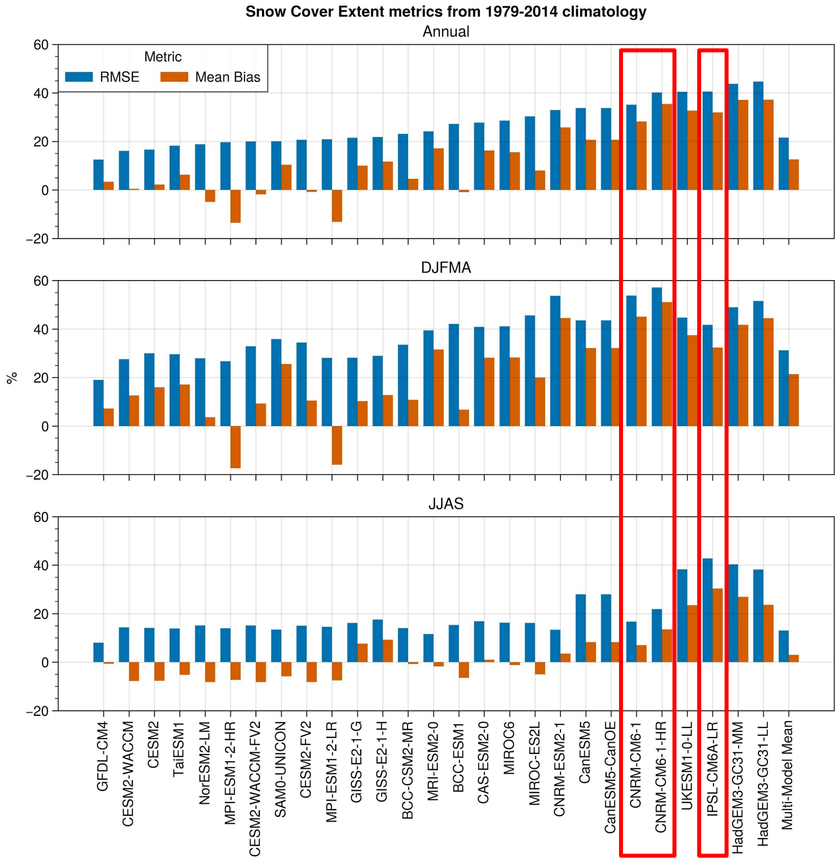

Precipitation

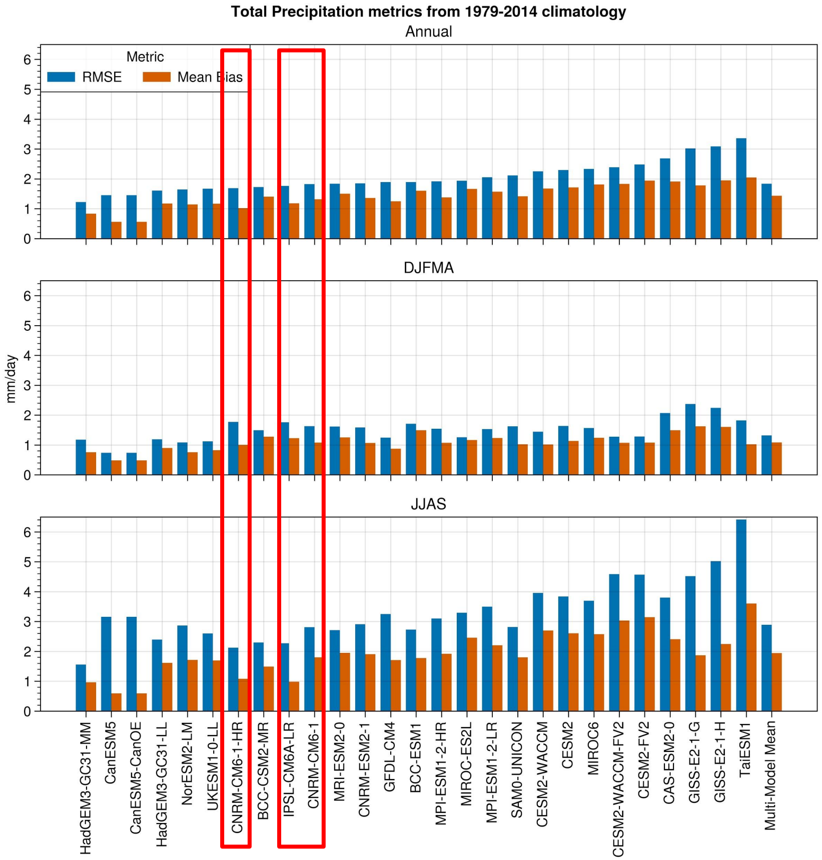

Atmospheric component of the IPSL integrated climate model LMDZ4